

# Relations between skin friction and other surface quantities in viscous flows <sup>EP</sup>

Cite as: Phys. Fluids **31**, 107101 (2019); <https://doi.org/10.1063/1.5120454>

Submitted: 18 July 2019 . Accepted: 11 September 2019 . Published Online: 01 October 2019

Tao Chen (陈涛) , Tianshu Liu (刘天舒) , Lian-Ping Wang (王连平) , and Shiyi Chen (陈十一)

## COLLECTIONS

 This paper was selected as an Editor's Pick



View Online



Export Citation



CrossMark

## ARTICLES YOU MAY BE INTERESTED IN

[The theory and application of Navier-Stokeslets \(NSlets\)](#)

Physics of Fluids **31**, 107103 (2019); <https://doi.org/10.1063/1.5119331>

[Boundary layer turbulence and freestream turbulence interface, turbulent spot and freestream turbulence interface, laminar boundary layer and freestream turbulence interface](#)

Physics of Fluids **31**, 045104 (2019); <https://doi.org/10.1063/1.5093040>

[Wall-attached clusters for the logarithmic velocity law in turbulent pipe flow](#)

Physics of Fluids **31**, 055109 (2019); <https://doi.org/10.1063/1.5096433>

AIP Author Services  
English Language Editing



# Relations between skin friction and other surface quantities in viscous flows

Cite as: Phys. Fluids 31, 107101 (2019); doi: 10.1063/1.5120454

Submitted: 18 July 2019 • Accepted: 11 September 2019 •

Published Online: 1 October 2019



View Online



Export Citation



CrossMark

Tao Chen (陈涛),<sup>1</sup>  Tianshu Liu (刘天舒),<sup>2,3,a)</sup>  Lian-Ping Wang (王连平),<sup>2,4</sup>  and Shiyi Chen (陈十一)<sup>1,2</sup>

## AFFILIATIONS

<sup>1</sup>SKLTCS, College of Engineering, Peking University, Beijing 100871, People's Republic of China

<sup>2</sup>Department of Mechanics and Aerospace Engineering, Southern University of Science and Technology, Shenzhen, China

<sup>3</sup>Department of Mechanical and Aerospace Engineering, Western Michigan University, Kalamazoo, Michigan 49008, USA

<sup>4</sup>Department of Mechanical Engineering, University of Delaware, Newark, Delaware 19716, USA

<sup>a)</sup> Author to whom correspondence should be addressed: [tianshu.liu@wmich.edu](mailto:tianshu.liu@wmich.edu)

## ABSTRACT

This paper presents the derivations of the exact relations between skin friction and other important dynamical and kinematical quantities on a stationary curved surface in a viscous flow by applying the standard methods of differential geometry to the governing partial differential equations in fluid mechanics. In particular, the mathematical structures of the effects of the surface curvature are explicitly expressed, which extend the previous results on a flat surface. These relations reveal that skin friction is intrinsically coupled with surface pressure, temperature, and scalar concentration through the boundary enstrophy flux, heat flux, and mass flux, respectively. As an example, the relation between skin friction and surface pressure is examined in the Oseen flow over a sphere to elucidate the significant effect of the surface curvature at a very small Reynolds number. Two other validation examples are a gravity-driven creeping liquid film flow over a wavy surface and the Falkner-Skan flow over a wedge. Furthermore, the relation is applied to a simulated turbulent channel flow to explore the local near-wall coherent structure and understand its dynamical roles in turbulence production.

Published under license by AIP Publishing. <https://doi.org/10.1063/1.5120454>

## I. INTRODUCTION

Skin friction (conventionally denoted by  $\tau$ ) is the wall shear stress defined as the derivative of the velocity multiplying the dynamic viscosity in the wall-normal direction at a solid surface, which is a major contributor to the fluid-mechanic drag. Skin friction vector fields reveal the complex flow topology particularly in three-dimensional (3D) separated flows and turbulent boundary layers.<sup>1–8</sup> In particular, near-wall flow structures in separated flows and turbulent flows are determined by the skin friction field and the surface pressure field.<sup>9–12</sup> Conventionally, skin friction is treated as an independent quantity, and therefore, the direct connections between skin friction and other surface quantities are not sufficiently studied. In fact, there are the explicit coupling relations between skin friction and other important surface quantities, particularly surface pressure, surface temperature, and surface scalar concentration. These relations are useful in the following aspects. From a theoretical perspective, the coupling structures of skin friction and other surface

quantities provide a useful tool to identify and understand coherent near-wall structures in complex flows. On the other hand, from a standpoint of measurement, the coupling relations between skin friction and other more measurable surface quantities can be used to extract high-resolution skin friction fields as an inverse problem from surface flow visualizations. This work focuses on the exact relations between skin friction and other surface quantities and their applications. The previous developments on this topic are briefly reviewed below.

To study the feasibility of extracting a skin friction field from global surface pressure measurement, the Navier-Stokes (NS) equations on a surface was recast by Liu *et al.*<sup>13</sup> into a form of the optical flow equation. They gave a relation between skin friction ( $\tau$ ) and surface pressure ( $p_{\partial B}$ ) on a surface in an incompressible flow, which is given by  $\tau \cdot \nabla_{\partial B} p_{\partial B} = \mu f_{\Omega}$ , where  $f_{\Omega}$  is interpreted as the boundary enstrophy flux (BEF) plus the curvature-induced contribution (see Appendix A),  $\nabla_{\partial B}$  is the gradient operator on the surface,  $\mu$  is the dynamic viscosity of fluid, and the subscript

$\partial B$  denotes the property on the surface. The derivation of this relation is based on the Taylor-series expansion of a velocity field in the wall-normal coordinate in the NS equations near a surface and the use of the geometric properties of a vorticity line on the surface. The relation represents an intrinsic coupling between skin friction and surface pressure through the BEF. This relation has been used for extraction of skin friction fields from pressure-sensitive-paint (PSP) measurements, elucidation of the role of the fluid viscosity in lift generation, and reconstruction of near-wall flow structures.<sup>14,15</sup>

Similarly, to establish the relation between skin friction, surface temperature, and heat flux, the energy equation was recast,<sup>16</sup> which leads to a relation  $\boldsymbol{\tau} \cdot \nabla_{\partial B} T_{\partial B} = \mu f_Q$ , where  $T_{\partial B}$  is the surface temperature and  $f_Q$  is related to the heat flux and the third-order normal derivative of the temperature at the surface, the curvature term, and the viscous dissipation term (see Appendix B). In certain sense, this relation is a general differential form of the Reynolds analogy between the skin friction and boundary heat flux, which has been used for extraction of skin friction fields from temperature-sensitive-paint (TSP) measurements in air flows<sup>16</sup> and water flows.<sup>17</sup> Since the mass transfer process is similar to the heat transfer process, a relation between skin friction and surface scalar concentration ( $\phi_{\partial B}$ ) was derived from the mass transport equation, which is  $\boldsymbol{\tau} \cdot \nabla_{\partial B} \phi_{\partial B} = \mu f_M$ , where  $f_M$  is related to the mass flux and the third-order normal derivative of the surface scalar concentration at the surface, the curvature term, and the source term. This relation has been used for extraction of skin friction fields from mass transfer visualizations using PSP and sublimation and dye coatings.<sup>18,19</sup>

These relations have a generic form of  $\boldsymbol{\tau} \cdot \nabla_{\partial B} g = f$ , where  $g$  is a measurable quantity,  $f$  can be measured or modeled, and  $\nabla_{\partial B}$  is the gradient operator on a surface (or the image plane after projection). From mathematical perspective, the determination of the vector field  $\boldsymbol{\tau}$  from the given fields of  $g$  and  $f$  is an inverse problem similar to the optical flow problem in computer vision. The classical optical flow equation in the image plane is written as  $\mathbf{u} \cdot \nabla g = f$ , where  $g$  is the image intensity,  $f = -\partial g / \partial t$  is the negative time derivative of  $g$ , and  $\mathbf{u}$  is the optical flow that is the velocity of a moving object in the physical space projected onto the image plane. Therefore, the variational method is adopted to solve this problem in the image plane for extraction of a skin friction field from surface flow visualizations.<sup>14-19</sup>

However, the previous studies do not sufficiently discuss the effects of the surface curvature in the coupling relations. From a theoretical standpoint, it is necessary to express the full mathematical structures of the effects of the surface curvature to determine whether these effects can be neglected in applications. In this work, we extend the previous results by providing more rigorous derivations of these relations on a general curved surface in the framework of differential geometry. The differential-geometric approach is applicable to a general curved surface, which is different from the previous Taylor-series-expansion approach for a flat surface. First, the coupling relation between skin friction and surface pressure is discussed, where a scalar quantity linking them contains the BEF (usually the dominant term), the curvature term, and the dilation rate term. This relation is derived from the NS equations for a viscous flow in Appendix A. The Oseen flow over a sphere is considered as an example for

elucidation in Appendix A, and the Oseen solution at small Reynolds number indeed satisfies this relation, where the effects of the surface curvature are significant. Next, the relation between skin friction and surface temperature is discussed, where a scalar quantity linking them contains the source term, the curvature term, and the dissipation rate term. This relation is derived from the energy equation in Appendix B, which is examined in the Falkner-Skan flow on an adiabatic wedge. Furthermore, the relation between skin friction and surface scalar concentration is similarly given, which is derived from the mass transport equation. Since these relations enjoy the same mathematical form of the optical flow equation, an inverse problem can be solved by using the variational method for extraction of a skin friction field from the measurable quantities. Furthermore, in an example of applying the relation between skin friction and surface pressure, the local structure called the hill-valley pocket (HVP) in a simulated turbulent channel flow is identified. From the snapshot surface pressure and BEF fields, the skin friction topology of the HVP is reconstructed. It is found that the HVP induces the high snapshot turbulent kinetic energy and Reynolds stress, which could play a significant role in generating stream-wise vortices and long streaks with high local skin friction magnitudes. The mathematical results used in the derivations are given in Appendix C.

## II. RELATION BETWEEN SKIN FRICTION AND SURFACE PRESSURE

The intrinsic relation between the skin friction vector  $\boldsymbol{\tau}$  and the surface pressure gradient  $\nabla_{\partial B} p_{\partial B}$  is derived from the Navier-Stokes (NS) equations with the no-slip boundary condition in a general surface coordinate system (see Appendix A). This relation is written in a vector form, i.e.,

$$\boldsymbol{\tau} \cdot \nabla_{\partial B} p_{\partial B} = \mu f_{\Omega}, \quad (1)$$

where  $f_{\Omega}$  acts as a virtual source term, which is expressed as

$$f_{\Omega} = \mu \left[ \frac{\partial \Omega}{\partial n} \right]_{\partial B} - \mu \boldsymbol{\omega}_{\partial B} \cdot \mathbf{K} \cdot \boldsymbol{\omega}_{\partial B} + \mu_{\theta} (\boldsymbol{\omega}_{\partial B} \times \mathbf{n}) \cdot \nabla_{\partial B} \theta_{\partial B}, \quad (2)$$

where  $\Omega = |\boldsymbol{\omega}|^2 / 2$  is the enstrophy,  $\partial / \partial n$  is the derivative along the normal direction,  $\boldsymbol{\omega} = \nabla \times \mathbf{u}$  is the vorticity,  $\mathbf{K} = b_{\alpha\beta} \mathbf{g}^{\alpha} \otimes \mathbf{g}^{\beta}$  is the surface curvature tensor,  $\theta = \nabla \cdot \mathbf{u}$  is the dilation rate,  $\mu$  is the dynamic viscosity,  $\mu_{\theta}$  is the longitudinal viscosity, and  $\mathbf{n}$  is the unit normal vector of the surface. The subscript  $\partial B$  in the variables and operators in Eqs. (1) and (2) denotes the quantities on the surface.

Equation (1) represents a formal balance between  $\nabla_{\partial B} p_{\partial B}$  projected on the skin friction vector  $\boldsymbol{\tau}$  and the scalar quantity  $f_{\Omega}$  that is originated from the diffusion term in the NS equations. In Eq. (2), the first term  $\mu [\partial \Omega / \partial n]_{\partial B}$  is the boundary enstrophy flux (BEF) and the second term is interpreted as the curvature-induced contribution. The term  $\boldsymbol{\omega}_{\partial B} \cdot \mathbf{K} \cdot \boldsymbol{\omega}_{\partial B}$  in Eq. (2) is formally interpreted as the interaction between the surface curvature and the vorticity on the surface. The quadratic form  $\boldsymbol{\omega}_{\partial B} \cdot \mathbf{K} \cdot \boldsymbol{\omega}_{\partial B}$  can be transformed into the standard form  $\boldsymbol{\omega}_{\partial B} \cdot \mathbf{K} \cdot \boldsymbol{\omega}_{\partial B} = \kappa_1 \omega_1^2 + \kappa_2 \omega_2^2$  with the two principal curvatures  $\kappa_1$  and  $\kappa_2$ , where  $\omega_1 = \boldsymbol{\omega}_{\partial B} \cdot \mathbf{e}_1$  and  $\omega_2 = \boldsymbol{\omega}_{\partial B} \cdot \mathbf{e}_2$  are the vorticity components on the principal directions  $\mathbf{e}_1$  and  $\mathbf{e}_2$ . For a concave surface with  $\kappa_1 \leq 0$  and  $\kappa_2 < 0$  (such as concave

ellipsoid and cylinder),  $\boldsymbol{\omega}_{\partial B} \cdot \mathbf{K} \cdot \boldsymbol{\omega}_{\partial B} < 0$ . For a convex surface with  $\kappa_1 \geq 0$  and  $\kappa_2 > 0$  (such as convex ellipsoid and cylinder),  $\boldsymbol{\omega}_{\partial B} \cdot \mathbf{K} \cdot \boldsymbol{\omega}_{\partial B} > 0$ . For a hyperboloid surface with  $\kappa_1 > 0$  and  $\kappa_2 < 0$ , the sign of  $\boldsymbol{\omega}_{\partial B} \cdot \mathbf{K} \cdot \boldsymbol{\omega}_{\partial B}$  is undetermined. The ratio between the magnitudes of the second and first terms (the curvature and BEF terms) in Eq. (2) is proportional to  $\delta_c/R_s$ , where  $\delta_c$  is the viscous diffusion length scale and  $R_s$  is defined as the mean curvature radius of the surface. When the Reynolds number is sufficiently large such that  $\delta_c/R_s \ll 1$ , the second term in Eq. (2) could be neglected. In this case,  $f_\Omega$  is dominated by the BEF. The third term is interpreted as the contribution induced by the temporal-spatial change in the fluid density on the surface. According to the continuity equation  $\partial\rho/\partial t + \mathbf{u} \cdot \nabla\rho + \rho\nabla \cdot \mathbf{u} = 0$ , the term  $\nabla_{\partial B}\theta_{\partial B} = \nabla_{\partial B}[-\partial \ln \rho/\partial t]_{\partial B}$  represents the spatial and temporal change in the logarithm of the density on  $\partial B$ . For an unsteady compressible flow on a moving surface, the dilation rate  $\theta_{\partial B} \neq 0$  since the fluid density on  $\partial B$  may change temporally and spatially. However, for an unsteady incompressible flow or a steady compressible flow,  $\theta_{\partial B} = 0$ . Note that when the body force is not zero, the pressure  $p$  in Eq. (1) should be replaced by  $p + \varphi$ , where  $\varphi$  is the potential of the conservative body force (see an example in Appendix A 3).

Originally, considering the geometry of a vorticity line on the surface (referred to as a boundary vorticity line that is a tangent line to the vorticity  $\boldsymbol{\omega}_{\partial B}$  on the surface), Liu *et al.*<sup>13</sup> gave Eq. (1) with  $f_\Omega = \mu[\partial\Omega/\partial n]_{\partial B} - 2\mu\kappa_\omega\Omega_{\partial B}(\mathbf{n} \cdot \mathbf{n}_\omega)$ , where  $\kappa_\omega$  is the curvature of the boundary vorticity line and  $\mathbf{n}_\omega$  is the principal unit normal vector of the boundary vorticity line on  $\partial B$ . A question is

whether  $\boldsymbol{\omega}_{\partial B} \cdot \mathbf{K} \cdot \boldsymbol{\omega}_{\partial B}$  in Eq. (2) is equivalent to  $|\boldsymbol{\omega}_{\partial B}|^2 \kappa_\omega \mathbf{n}_\omega \cdot \mathbf{n}$ , where  $\boldsymbol{\omega}_{\partial B}$  is the boundary vorticity. Since the curve is constrained by the surface, its geometric quantities must be related to the surface. In differential geometry, there is a relation  $\kappa_{curve} \mathbf{n}_{curve} \cdot \mathbf{n} = b_{ij}(dx^i/ds)(dx^j/ds) = \mathbf{T} \cdot \mathbf{K} \cdot \mathbf{T}$ , where  $\kappa_{curve}$  is the curvature of the curve on the surface,  $\mathbf{n}_{curve}$  is the unit normal vector of the curve,  $\mathbf{n}$  is the normal vector of the surface at the same location,  $(ds)^2 = g_{ij}dx^i dx^j$  is the differential arc length squared,  $\mathbf{T}$  is the tangent vector of the curve, and  $\mathbf{K}$  is the curvature tensor.<sup>20</sup> In this paper, following the notations in differential geometry, we use  $x^i$  ( $i = 1, 2, 3$ ) as the coordinates on a surface, where  $(x^1, x^2)$  are the surface coordinates and  $x^3$  is the coordinate normal to the surface. Obviously, the tangent vector of the curve is in the tangent plane of the surface. Applying this relation to the vorticity line on the stationary surface with  $\mathbf{T} = \boldsymbol{\omega}_{\partial B}/|\boldsymbol{\omega}_{\partial B}|$ , we know  $\kappa_\omega \mathbf{n}_\omega \cdot \mathbf{n} = \boldsymbol{\omega}_{\partial B} \cdot \mathbf{K} \cdot \boldsymbol{\omega}_{\partial B}/|\boldsymbol{\omega}_{\partial B}|^2$ . According to this relation, the term  $\boldsymbol{\omega}_{\partial B} \cdot \mathbf{K} \cdot \boldsymbol{\omega}_{\partial B}$  can be interpreted as the projection of the boundary-vorticity-line curvature vector  $|\boldsymbol{\omega}_{\partial B}|^2 \kappa_\omega \mathbf{n}_\omega$  onto the surface normal vector. The factor  $\mathbf{n}_\omega \cdot \mathbf{n} = \boldsymbol{\omega}_{\partial B} \cdot \mathbf{K} \cdot \boldsymbol{\omega}_{\partial B}/(\kappa_\omega |\boldsymbol{\omega}_{\partial B}|^2)$  is the cosine of the angle between the unit normal vector  $\mathbf{n}_\omega$  of the boundary vorticity line and the normal vector  $\mathbf{n}$  of the surface. It is noted that a constraint  $\mathbf{n}_\omega \cdot \mathbf{n} = 1$  was used for an upper bound estimation of the curvature term.<sup>13</sup> In general, the principal unit normal vector  $\mathbf{n}_\omega$  of a curve on a surface is not aligned with the normal unit vector  $\mathbf{n}$  of the surface ( $\mathbf{n}_\omega \cdot \mathbf{n} \leq 1$ ) since the curve could be bent on the surface. Thus, an inequality  $|\boldsymbol{\omega}_{\partial B} \cdot \mathbf{K} \cdot \boldsymbol{\omega}_{\partial B}| \leq \kappa_\omega |\boldsymbol{\omega}_{\partial B}|^2$  holds. The present analysis based on the surface itself is consistent with

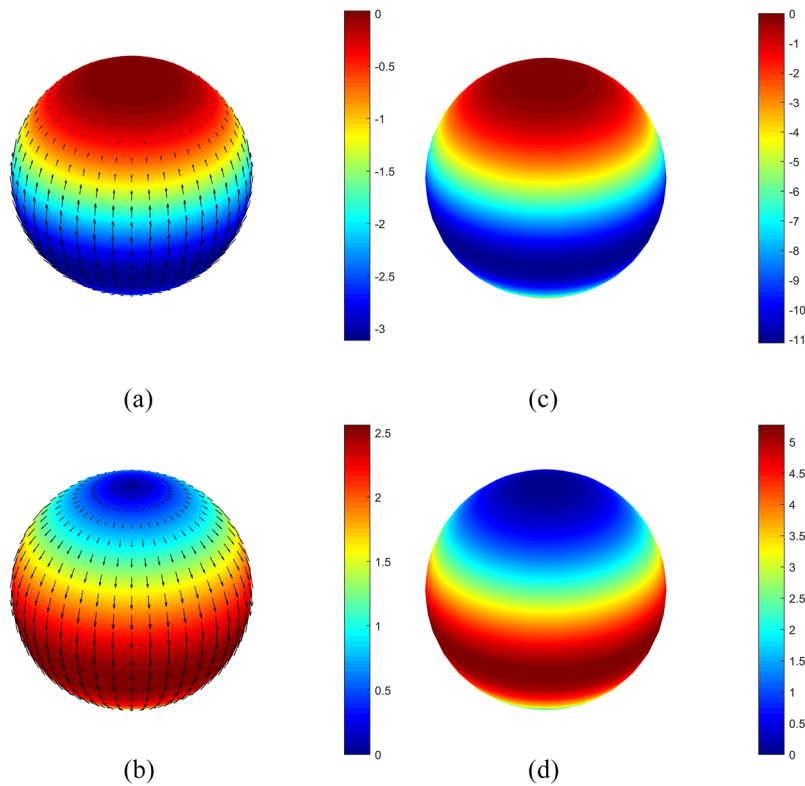


FIG. 1. Distributions of the normalized surface quantities on a sphere in the Oseen flow at a low Reynolds number ( $Re = 1.5$ ): (a) pressure gradient  $\nabla_{\partial B}\rho_{\partial B}/(\mu u_0/R^2)$ , (b) skin friction  $\tau/(\mu u_0/R)$ , (c) BEF  $[\partial\Omega/\partial r]_{r=R}/(u_0^2/R^3)$ , and (d) curvature term  $-\boldsymbol{\omega}_{\partial B} \cdot \mathbf{K} \cdot \boldsymbol{\omega}_{\partial B}/(u_0^2/R^3)$ . Flow is from top to bottom.

the previous analysis based on the geometrical properties of a curve on a surface.<sup>13</sup>

It is worth noting that Eq. (1) can be derived in a special reference frame called the  $\tau$ -frame by utilizing the fact that the skin friction lines and vorticity lines on a surface are orthogonal.<sup>5,21</sup> The  $\tau$ -frame is a natural orthonormal surface frame, in which the unit coordinate vectors are given by  $\mathbf{e}_1 = \boldsymbol{\tau}/\|\boldsymbol{\tau}\|$ ,  $\mathbf{e}_2 = \boldsymbol{\omega}_{\partial B}/\|\boldsymbol{\omega}_{\partial B}\|$ , and  $\mathbf{e}_3 = \mathbf{e}_1 \times \mathbf{e}_2 = \mathbf{n}$ . In this case, the curvature term in  $f_\Omega$  can be written as

$$\begin{aligned} -\mu\boldsymbol{\omega}_{\partial B} \cdot \mathbf{K} \cdot \boldsymbol{\omega}_{\partial B} &= -\mu|\boldsymbol{\omega}_{\partial B}|e_2 \cdot b_{\alpha\beta}\mathbf{e}_\alpha \otimes \mathbf{e}_\beta \cdot |\boldsymbol{\omega}_{\partial B}|e_2 \\ &= -\mu|\boldsymbol{\omega}_{\partial B}|^2 b_{22} = -2b_{22}\mu\Omega_{\partial B}, \end{aligned} \quad (3)$$

where  $b_{\alpha\beta}$  ( $\alpha, \beta = 1, 2$ ) are the coefficients of the surface curvature tensor  $\mathbf{K}$  (see Appendix A).

To elucidate the above theoretical result particularly the effect of the surface curvature, the steady flow over a sphere at low Reynolds numbers (the Oseen flow) is given as an example in Appendix A. It is found that Eq. (1) holds up to the order of  $O(\text{Re})$  in the Oseen solution. Figure 1 shows the distributions of the relevant normalized surface quantities on a sphere at low Reynolds numbers. In the Oseen flow over a sphere, the pressure gradient  $\nabla_{\partial B} p_{\partial B}/(\mu u_0/R^2)$  has the opposite direction of the skin friction  $\boldsymbol{\tau}/(\mu u_0/R)$ . The BEF term  $[\partial\Omega/\partial r]_{r=R}/(u_0^2/R^3)$  is negative, while the curvature term  $-\boldsymbol{\omega}_{\partial B} \cdot \mathbf{K} \cdot \boldsymbol{\omega}_{\partial B}/(u_0^2/R^3)$  is positive due to the concavity of the surface. The magnitudes of the BEF and curvature terms are comparable since the viscous diffusion length scale is of the same order as the curvature radius. Therefore, the effect of the surface curvature could be significant when the Reynolds number is very small.

### III. RELATION BETWEEN SKIN FRICTION AND SURFACE TEMPERATURE

The relation between the skin friction vector  $\boldsymbol{\tau}$  and the surface temperature  $T_{\partial B}$  is derived from the energy equation (see Appendix B). This relation is written as

$$\boldsymbol{\tau} \cdot \nabla_{\partial B} T_{\partial B} = \mu f_Q, \quad (4)$$

where the virtual source term is given by

$$\begin{aligned} f_Q &= \frac{1}{k} \left( \frac{\partial}{\partial t} - a\nabla_{\partial B}^2 \right) q_{\partial B} + \frac{\mu}{\rho c} \left[ \frac{\partial \Phi}{\partial x^3} \right]_{\partial B} - 2aH_{mean} \left[ \frac{\partial^2 T}{\partial (x^3)^2} \right]_{\partial B} \\ &+ a \left[ \frac{\partial^3 T}{\partial (x^3)^3} \right]_{\partial B} + a[\mathbf{K} : \mathbf{K} q_{\partial B}/k + 2\text{Tr}(\nabla_{\partial B} \nabla_{\partial B} T_{\partial B} \cdot \mathbf{K}) \\ &+ (\nabla_{\partial B} \cdot \mathbf{K}) \cdot (\nabla_{\partial B} T_{\partial B})]. \end{aligned} \quad (5)$$

In Eq. (5),  $\rho$  is the density of the fluid,  $c$  is the specific heat,  $T$  is the temperature,  $\mathbf{u}$  is the velocity of the fluid,  $p$  is the pressure,  $\mu$  is the dynamic viscosity,  $\Phi$  is the dissipation function,  $a = k/\rho c$  is the thermal diffusivity,  $H_{mean}$  is the mean curvature of the surface,  $\text{Tr}$  denotes the trace, and  $q_{\partial B} = -k[\partial T/\partial x^3]_{\partial B}$  is the heat flux on the surface which is positive when the heat enters into fluid from the surface. The term  $(\partial/\partial t - a\nabla_{\partial B}^2)q_{\partial B}$  in Eq. (5) is interpreted as a source term in the formal diffusion process of the heat flux on the surface. Equation (4) with suitable modeling of  $f_Q$  can be

used to study the skin friction topology in complex flows.<sup>16,17</sup> Here,  $T_{\partial B}$  is a quantity to be determined experimentally or computationally, which is not given as a boundary condition. The meaning of the term  $\nabla_{\partial B} \nabla_{\partial B} T_{\partial B}$  in Eq. (5) is discussed in Appendix B. Also, in Appendix B, Eq. (4) is validated in the Falkner-Skan flow as an example.

### IV. RELATION BETWEEN SKIN FRICTION AND SURFACE SCALAR CONCENTRATION

Similar to Eq. (4), the relation between skin friction and surface scalar concentration is derived from the binary mass diffusion equation with a source term, i.e.,<sup>23</sup>

$$\partial\phi/\partial t + \mathbf{u} \cdot \nabla\phi = D_{12}\nabla^2\phi + Q_s, \quad (6)$$

where  $\phi = \rho_1/\rho$  is the relative concentration (density) of species 1,  $\rho = \rho_1 + \rho_2$  is the total density of the binary gas,  $D_{12}$  is the diffusivity of a binary system, and  $Q_s$  is the source term. Since Eq. (6) has the same mathematical structure as the energy equation, following the same procedure in Appendix B, we have

$$\boldsymbol{\tau} \cdot \nabla_{\partial B} \phi_{\partial B} = \mu f_M, \quad (7)$$

where the virtual source term is written as

$$\begin{aligned} f_M &= \frac{1}{D_{12}\rho_{\partial B}} \left( \frac{\partial}{\partial t} - D_{12}\nabla_{\partial B}^2 \right) \dot{m}_{1\partial B} + \left[ \frac{\partial Q_s}{\partial x^3} \right]_{\partial B} \\ &- 2D_{12}H_{mean} \left[ \frac{\partial^2 \phi}{\partial (x^3)^2} \right]_{\partial B} + D_{12} \left[ \frac{\partial^3 \phi}{\partial (x^3)^3} \right]_{\partial B} \\ &+ [\mathbf{K} : \mathbf{K} \dot{m}_{1\partial B}/\rho_{\partial B} + 2D_{12} \text{Tr}(\nabla_{\partial B} \nabla_{\partial B} \phi_{\partial B} \cdot \mathbf{K}) \\ &+ D_{12}(\nabla_{\partial B} \cdot \mathbf{K}) \cdot (\nabla_{\partial B} \phi_{\partial B})], \end{aligned} \quad (8)$$

and  $\dot{m}_{1\partial B} = -D_{12}\rho_{\partial B}[\partial\phi/\partial x^3]_{\partial B}$  is the diffusive flux of species 1 on the surface. The term  $(\partial/\partial t - D_{12}\nabla_{\partial B}^2)\dot{m}_{1\partial B}$  in Eq. (8) is interpreted as a source term in the formal diffusion process of the mass flux on the surface. Equation (7) with suitable modeling of  $f_M$  was used to study the skin friction topology on delta wings in a water flow based on surface luminescent dye visualizations.<sup>19</sup> Equation (7) is validated in the Falkner-Skan flow in Appendix B.

### V. VARIATIONAL METHOD

Based on the basic relations given in Secs. II–IV, an inverse problem is to determine the skin friction field from the measured surface pressure, temperature, and scalar concentration fields in global surface flow diagnostics. Since global flow diagnostics are essentially image-based measurements, this problem is conveniently solved from a perspective of image processing such as the well-known optical flow problem.<sup>24,25</sup> For image processing, the basic equations should be projected onto the image plane through one-to-one mapping between the surface coordinates and the image coordinates. For simplicity, the orthographical projection mapping is considered here. The main equations, Eqs. (1), (4), and (7), can be projected onto the image plane and recast to a generic form, i.e.,

$$\boldsymbol{\tau} \cdot \nabla g = \mu f, \quad (9)$$

where  $\boldsymbol{\tau} = (\tau_1, \tau_2)$  is the skin friction vector projected on the image plane,  $g$  is a measurable quantity (e.g., surface pressure, temperature, and scalar concentration), the source term  $f$  is measured or modeled,  $\nabla = \partial/\partial x_i$  ( $i = 1, 2$ ) is the gradient operator in the image plane (projection of  $\nabla_{\partial B}$ ), and  $x_i$  are the image coordinates. To solve Eq. (9) as an inverse problem, the variational method is applied by minimizing the residue functional

$$J(\boldsymbol{\tau}) = \|\boldsymbol{\tau} \cdot \nabla g - \mu f\|_2 + \alpha \left( \|\nabla \tau_1\|^2 + \|\nabla \tau_2\|^2 \right), \quad (10)$$

where  $\|\cdot\|_2$  denotes the L2 norm on a domain  $D$  and  $\alpha$  is a Lagrange multiplier (a regularization parameter). The first term in  $J(\boldsymbol{\tau})$  is the equation term, and the second term is a regularization functional as a smoothness constraint assuming that a skin friction field is sufficiently continuous and smooth. The minimization of  $J(\boldsymbol{\tau})$  leads to the Euler-Lagrange equations, i.e.,

$$(\boldsymbol{\tau} \cdot \nabla g - \mu f) \nabla g - \alpha \nabla^2 \boldsymbol{\tau} = 0, \quad (11)$$

where  $\nabla^2 = \partial^2/\partial x_i \partial x_i$  ( $i = 1, 2$ ) is the Laplace operator in the image plane. Given the surface pressure and BEF fields, the Euler-Lagrange equations can be solved numerically for a skin friction field with the Neumann condition  $\partial \boldsymbol{\tau} / \partial n = 0$  on the domain boundary  $\partial D$ . The mathematical analysis of the optical flow is applicable to this problem.<sup>26–28</sup> The standard finite difference method is used to solve Eq. (11), and the numerical algorithms for the optical flow problem can be adapted.<sup>28</sup>

In an error analysis, the decompositions  $g = g_0 + \delta g$ ,  $f = f_0 + \delta f$ , and  $\boldsymbol{\tau} = \boldsymbol{\tau}_0 + \delta \boldsymbol{\tau}$  are introduced, where  $\delta g$ ,  $\delta f$ , and  $\delta \boldsymbol{\tau}$  are errors, and  $g_0$ ,  $f_0$ , and  $\boldsymbol{\tau}_0$  are the nonperturbed fields that exactly satisfy Eq. (11). Substituting the above decompositions into Eq. (11) and neglecting the higher-order small terms, we have an error propagation equation

$$(\delta \boldsymbol{\tau} \cdot \nabla g_0) \nabla g_0 - \alpha \nabla^2 \delta \boldsymbol{\tau} = -(\delta f + \boldsymbol{\tau}_0 \cdot \nabla \delta g) \nabla g_0, \quad (12)$$

where  $\delta f$  directly contributes to  $\delta \boldsymbol{\tau}$  and  $\delta g$  contributes to  $\delta \boldsymbol{\tau}$  through a gradient operator projected on the skin friction vector.

In a local linear approximation, we consider a local region where  $\nabla g_0$  is a constant vector with the magnitude  $\|\nabla g_0\|$  and introduce the unit normal vector to an isovalue line  $g_0 = \text{const}$ , i.e.,  $\mathbf{N}_T = \nabla g_0 / \|\nabla g_0\|$ . The skin friction error projected on  $\mathbf{N}_T$  is defined as  $(\delta \boldsymbol{\tau})_N = \delta \boldsymbol{\tau} \cdot \mathbf{N}_T$ . From Eq. (12), a formal estimate of the relative error is obtained, i.e.,

$$\frac{(\delta \boldsymbol{\tau})_N}{\|\boldsymbol{\tau}_0\|} = -\frac{\delta f}{\|\nabla g_0\| \|\boldsymbol{\tau}_0\|} - \left( \frac{\boldsymbol{\tau}_0}{\|\boldsymbol{\tau}_0\|} \right) \cdot \delta \mathbf{N}_T + \frac{\alpha}{\|\nabla g_0\|^2} \nabla^2 \left[ \frac{(\delta \boldsymbol{\tau})_N}{\|\boldsymbol{\tau}_0\|} \right], \quad (13)$$

where  $\|\boldsymbol{\tau}_0\|$  is a characteristic value of skin friction (e.g., the mean value). The first term in the right-hand side (RHS) of Eq. (13) is the contribution from  $\delta f$ , and the second term is the contribution from the elemental error in measurement of the surface gradient of the relative intensity. The third term represents the artificial diffusion of the error  $(\delta \boldsymbol{\tau})_N$  associated with the Lagrange multiplier.

Since the first and third terms in the RHS of Eq. (13) are proportional to  $\|\nabla g_0\|^{-1}$  and  $\|\nabla g_0\|^{-2}$ , respectively, the relative error  $(\delta \boldsymbol{\tau})_N / \|\boldsymbol{\tau}_0\|$  increases as  $\|\nabla g_0\|$  decreases. The proportional factor

$\alpha \|\nabla g_0\|^{-2}$  in the third term is interesting. It is indicated that when  $\|\nabla g_0\|$  is small, the Lagrange multiplier  $\alpha$  should be sufficiently small to reduce the error. On the other hand, for an ill-posed problem, the variational solution with the Lagrange multiplier  $\alpha$  is affected by the data error bounded by a positive number  $\delta$ . The selected value of  $\alpha$  depends on  $\delta$ , i.e.,  $\alpha = \alpha(\delta)$ . The error of the solution is proportional to  $\delta/\alpha$  as  $\delta \rightarrow 0$ .<sup>29,30</sup> The condition for the solution convergence is  $\delta^2/\alpha(\delta) \rightarrow 0$ , indicating that the data error must be reduced when  $\alpha$  is small. Therefore, two conflicting requirements exist in the case. In the regions where  $\|\nabla g_0\|$  is small,  $\alpha$  should be small based on Eq. (13), and accordingly, the data error bound  $\delta$  must be tightly controlled to insure the accuracy of the solution. From this perspective, there may be the optimum value of the Lagrange multiplier. No rigorous theory is available to determine *a priori* the optimum value of the Lagrange multiplier. The selection of the Lagrange multiplier is a trial-and-error procedure based on simulations for a specific application. In Sec. VI, the optimum value of the Lagrange multiplier is determined in simulations.

## VI. LOCAL NEAR-WALL STRUCTURES IN TURBULENT CHANNEL FLOW

In this section, the application of Eq. (1) is demonstrated for identification and characterization of near-wall coherent structures in a turbulent channel flow. A different perspective is given by examining the intrinsically coupling structures of skin friction, surface pressure, BEF, and derived quantities in a simulated turbulent channel flow. The fully developed turbulent flow in a channel has been used as a canonical flow (along with turbulent boundary layer) to study the coherent structures in experiments and computational simulations.<sup>31–37</sup> Evidences of hairpin vortices are provided by measurements<sup>35,36</sup> and direct numerical simulations (DNSs).<sup>37–40</sup> There are some open questions on the coherent structures, including how they are objectively extracted (identified), how they are generated/regenerated, and how they are quantitatively related to the dynamical quantities in turbulence.

Direct numerical simulation (DNS) of a fully developed incompressible turbulent channel flow was conducted with the lattice Boltzmann method (LBM) at a frictional Reynolds number of  $Re_\tau = 180$  based on the channel half width  $H$  and the friction velocity.<sup>41</sup> Correspondingly, the bulk flow Reynolds number is  $Re_B = 2\bar{U}H/\nu \approx 5663$ , where  $\bar{U}$  is the mean flow velocity over the whole channel. The data set has been validated by comparing with benchmark data of the statistical properties of the flow in the literature.<sup>41,42</sup> In our LBM code, the viscous stress tensor  $\sigma_{ij}$  is directly obtained from the nonequilibrium part of the particle distribution function. The Chapman-Enskog expansion gives  $\sigma_{ij} = 2\mu(S_{ij} - \nabla \cdot \mathbf{u} \delta_{ij}/3) + \mu^V \nabla \cdot \mathbf{u} \delta_{ij}$ , where  $\mu$  is the shear viscosity and  $\mu^V$  is the bulk viscosity. Then, two-point (or three-point) Lagrange extrapolation is used to calculate skin-friction at a surface. For the surface pressure gradient, we first use two-point (or three point) Lagrange extrapolation to calculate surface pressure at a surface and then use a central difference scheme with the second-order accuracy to calculate the surface pressure gradient.

By examining the snapshot fields of the pressure variation and BEF on the bottom surface, it is found that notable features in

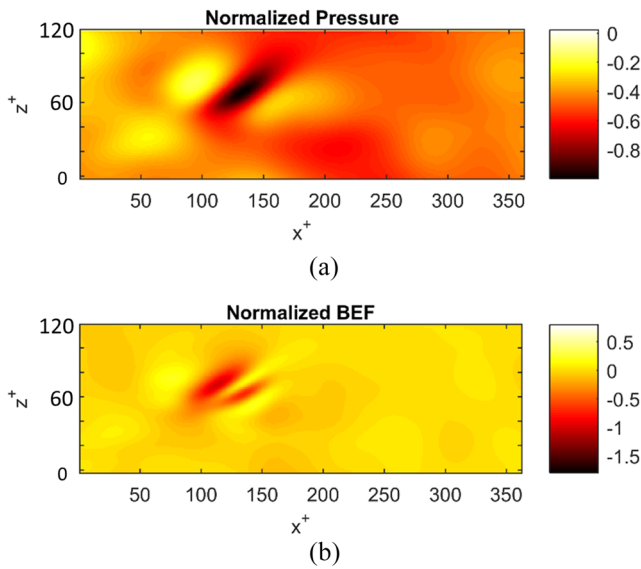


**FIG. 2.** Snapshot distributions normalized by the maximum value in the region of the HVP: (a) surface pressure and (b) BEF. Flow is from left to right.

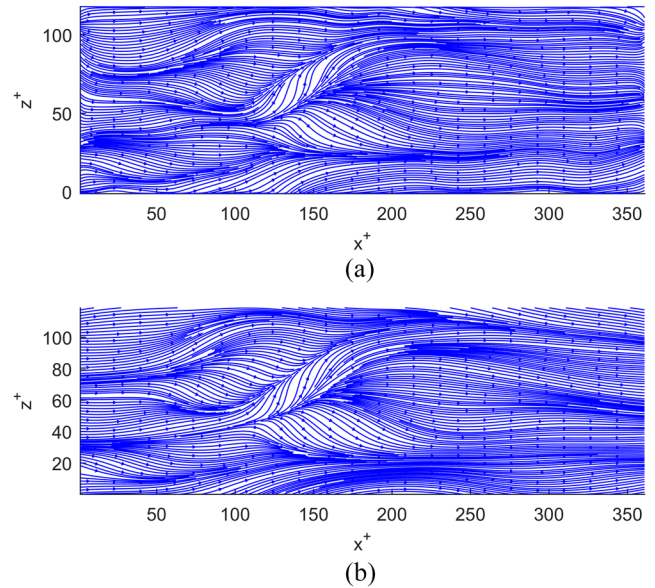


**FIG. 3.** Snapshot skin friction lines in the region of the HVP: (a) reconstructed field from the surface and BEF fields in Fig. 2 and (b) DNS. Flow is from left to right.

the surface variation are elongated pressure hills and valleys closely packed in those regions. For convenience, we call them hill-valley pockets (HVPs) (a topographical term). Figures 2(a) and 2(b) show the typical snapshot surface pressure and BEF images normalized by the maximum values in the region of a typical HVP, respectively. The large surface pressure variations in the turbulent channel flow are characterized by the HVPs that are highly intermittently distributed on the surface.

From the images in Fig. 2, the snapshot skin friction field is reconstructed by solving the Euler-Lagrange equations [Eq. (11)], in the image plane, and then mapped on the physical surface, where  $g = p_{\partial B}$  and  $f = f_{\Omega}$ . Figure 3(a) shows the reconstructed skin friction topology for the Lagrange multiplier of 0.1, which is consistent with that obtained in DNS in Fig. 3(b). The total root-mean-square (RMS) error in the whole region is evaluated by integrating the error distributions, i.e.,

$$Error = \frac{1}{mn} \sum_{i=1}^m \sum_{j=1}^n [(\tau_1(i,j) - \tau_{1,DNS}(i,j))^2 + (\tau_2(i,j) - \tau_{2,DNS}(i,j))^2]^{1/2}, \quad (14)$$

where  $\tau_1$  and  $\tau_2$  are the skin friction components in the main streamwise and spanwise directions, respectively,  $n$  and  $m$  are the numbers of the data points (pixels in the image plane) in the main streamwise and spanwise directions, respectively, and the subscript “DNS” denotes the DNS data. Figure 4 shows the relative errors in the extracted skin friction magnitude and angle as a function of the Lagrange multiplier ( $\alpha$ ), where the errors are normalized by the maximum magnitude and absolute directional angle. The relative error in the skin friction magnitude is at minimum of 0.23% for the Lagrange multiplier of 0.1, as indicated in the error analysis in Sec. V. In contrast, the relative error in the absolute directional

angle is about 23% when the Lagrange multiplier is less than 1. As shown in Fig. 3, there are several separation and attachment lines associated with the HVP. Here, a separation line is defined as a skin friction line to which all neighboring skin friction lines

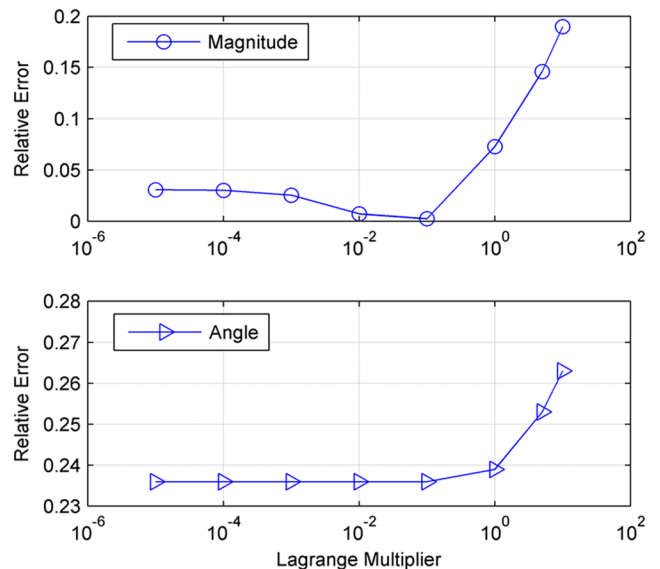


**FIG. 4.** The relative errors in the extracted skin friction magnitude and directional angle as a function of the Lagrange multiplier in the region shown in Fig. 3, where the errors are normalized by the maximum magnitude and absolute angle, respectively.

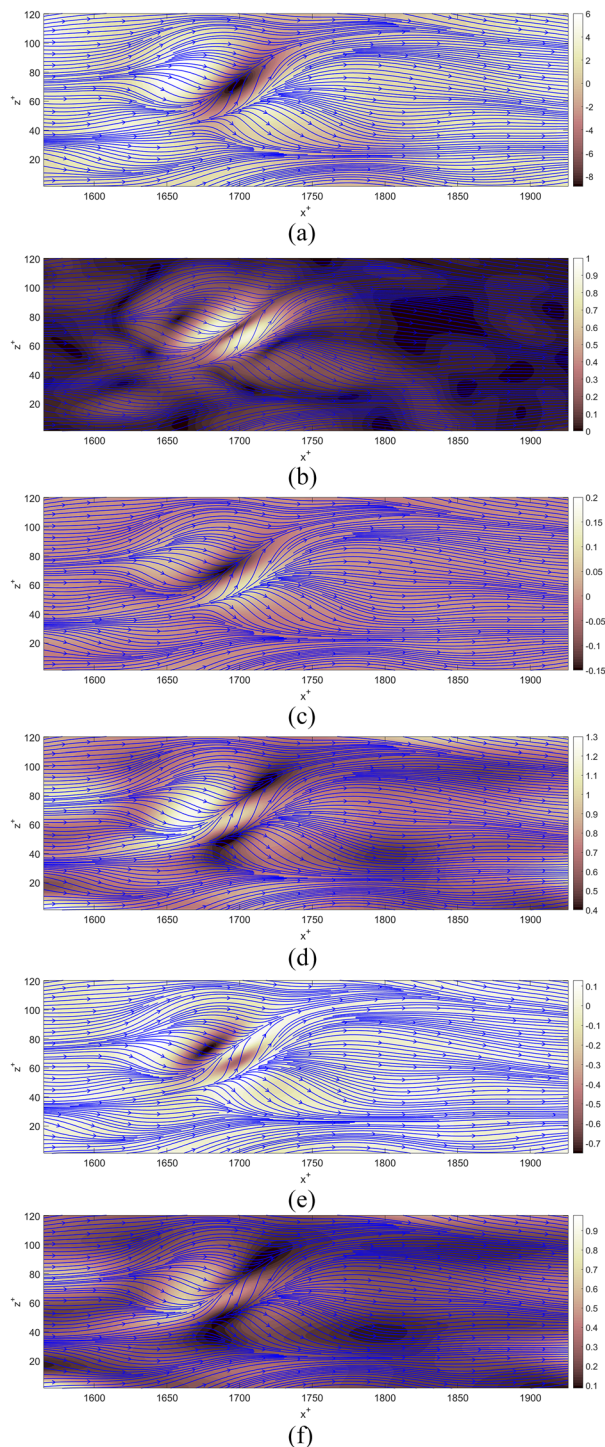


**FIG. 5.** Normalized snapshot fields of skin friction and other surface quantities in the region of the HVP: (a) skin friction and pressure ( $\tau^+, \delta p^+$ ), (b) skin friction and pressure gradient magnitude ( $\tau^+, \|\nabla_{\partial B^+} \rho_{\partial B^+}\|$ ), (c) skin friction and skin friction divergence ( $\tau^+, \tau_{\partial B^+} \cdot \nabla_{\partial B^+}$ ), (d) skin friction and its magnitude ( $\tau^+, \|\tau_{\partial B^+}\|$ ), (e) skin friction and BEF ( $\tau^+, \partial \Omega^+ / \partial n^+$ ), and (f) skin friction and enstrophy ( $\tau^+, \Omega^+$ ). Flow is from left to right.

converge, while an attachment line is a skin friction line from which all neighboring skin friction lines diverge. The surface pressure and skin friction features determine the near-wall flow structures of the HVP according to the Taylor-series-expansion solution of the NS equations.<sup>11,15</sup>

To examine the near-wall flow structures of the HVP, the fields of the relevant surface quantities are overlaid on the skin friction lines in Fig. 5. Figure 5(a) shows the snapshot surface pressure variation field of the HVP, indicating that the separation and attachment lines approximately correspond to the low and high surface pressure regions, respectively. The primary separation line is located in the valley of the surface pressure variation, while the two attachment lines are located on the two hills. The similar correspondence

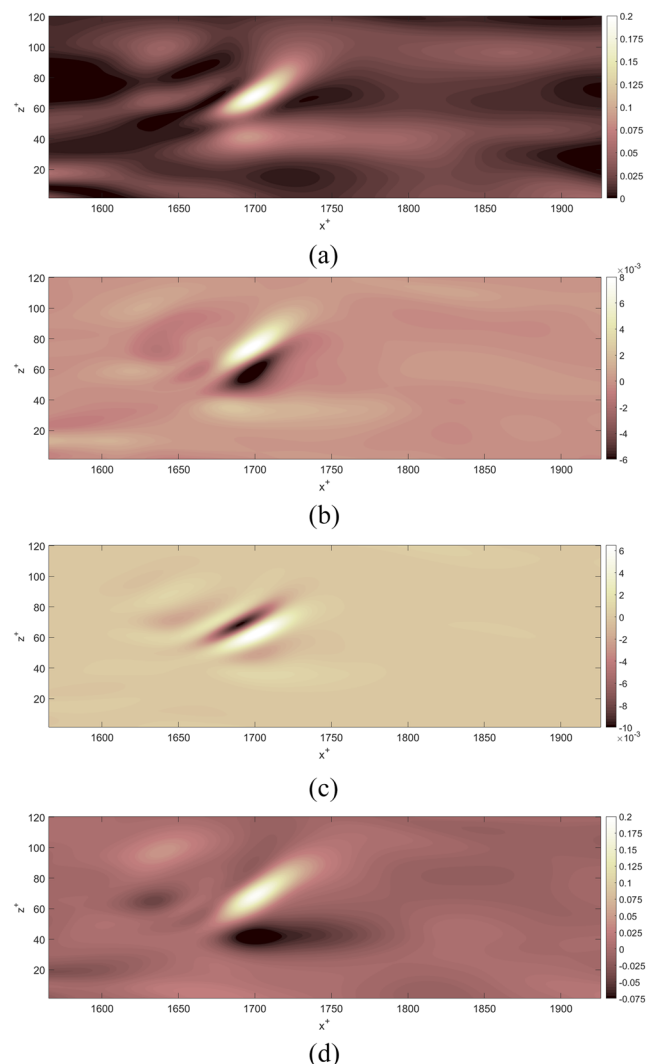


**FIG. 6.** Normalized snapshot fields of the turbulent activities of the HVP, (a) kinetic energy  $k^+ = (u'^+2 + v'^+2 + w'^+2)/2$ , (b) Reynolds stress component  $-u'v'$ , (c) Reynolds stress component  $-v'w'$ , and (d) Reynolds stress component  $-u'w'$ . Flow is from left to right.

between the separation/attachment lines and the topography of the surface pressure gradient magnitude is shown in Fig. 5(b). The skin friction divergence in Fig. 5(c) shows the correspondence between the negative divergence (the valley) and the separation line, inferring that there is the upward wall-normal velocity (upwelling) there. In contrast, the positive divergence (the hill) corresponds to the attachment line where there is the downward wall-normal velocity. The corresponding skin friction magnitude patterns are shown in Fig. 5(d). As indicated in Fig. 5(e), the HVP of the BEF field clearly corresponds to the skin friction topology. Relatively, the enstrophy pattern and the skin friction topology are less correlated in Fig. 5(f).

Figure 6 shows the snapshot fields of the turbulent kinetic energy and the three Reynolds stress components in the HVP at

$y^+ = 0.6$ . As shown in Fig. 6(a), the strong peak in the turbulent kinetic energy is located at the separation line where the strong upward wall-normal velocity is generated. In contrast, the peaks at the attachment lines are much weaker. As shown in Figs. 6(b) and 5(c), there are the positive hills and negative valleys in  $-u'^+v'^+$  and  $-v'^+w'^+$ , which are associated with the HVP. The positive hill of  $-u'^+v'^+$  is located at the separation line, which is similar to that in Fig. 6(a). It is further confirmed that the HVP in the surface pressure and BEF strongly contribute to the turbulence generation. Figure 7 shows the near-wall streamlines superposed on the enstrophy maps on cross sections, which are associated with the HVP, where the surface pressure map, BEF map, and skin friction lines are shown on the floor. A pair of the counter-rotating streamwise vortices is found at the height of about 20 wall units from the wall in the viscous sublayer. Such streamwise vortices in wall-bounded turbulent flows have been found in experiments and DNS.<sup>40–45</sup> The centers of the vortices in sections move upward slightly along the streamwise direction, and thus, the vortices are inclined slightly. The strong upward wall-normal velocity is induced by the pair of the vortices between them, which corresponds to the separation line between the surface pressure hills. The downward wall-normal velocity is induced by the vortices near the attachment lines. This pair of the streamwise vortices is consistent with the skin friction topology and the topographical features of the surface pressure, BEF, and other relevant surface quantities of the HVP.

Loosely speaking, coherent structures are highly correlated structures in the fields of the dynamical quantities (pressure and shear stresses) and kinematical quantities (velocity and its derived quantities such as vorticity, enstrophy, strain rate, and acceleration) in a 3D space and on a surface. Equation (1) imposes a deterministic (quasideterministic) on-wall constraint on near-wall coherent structures. The structures in the skin friction, surface pressure, and BEF fields are indeed correlated, and the turbulent activities relevant to these quantities are revealed. Furthermore, near-wall structures in the velocity and vorticity fields can be inferred by using the Taylor-series-expansion solution of the NS equations based on the skin friction and surface pressure structures. Therefore, Eq. (1) can potentially serve as a useful tool to study near-wall coherent structures.

## VII. CONCLUSIONS

The exact coupling relations between the skin friction and other surface quantities (pressure, temperature, and scalar concentration) are derived from the NS equations, energy equations, and mass transport equations in a general curvilinear coordinate system on a surface. These relations can be used to infer the skin friction topology in complex flows based on computations and measurements of pressure, temperature, and scalar concentration on a surface. The contribution of this work is that the mathematical structures of the effects of the surface curvature are explicitly expressed. As an analytical example, the relation between skin friction, surface pressure, and boundary enstrophy flux (BEF) is evaluated in the Oseen flow over a sphere, indicating the significant effects of the surface curvature in this low-Reynolds-number flow. Another example for validation is a gravity-driven creeping liquid film flow over a wavy surface. Furthermore, since skin friction, surface pressure, and

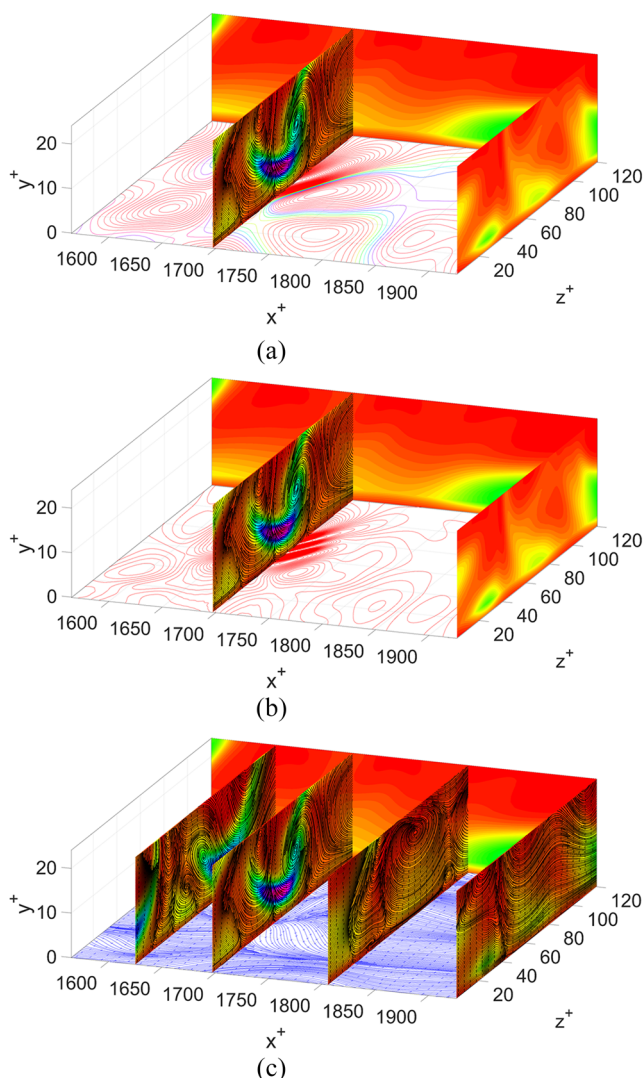


**FIG. 7.** Near-wall streamlines superposed on the enstrophy map on cross sections in the region of the HVP above (a) surface pressure map, (b) BEF map, and (c) skin friction lines. Here, the quantities are normalized by the wall units.

BEF constitute a group of the intrinsically coupled physical quantities, they can be used to understand the near-wall structures of complex flows. From this perspective, the DNS data of a turbulent channel flow are analyzed as a preliminary exploration. The local structure called the hill-valley pocket (HVP) in the surface pressure and BEF fields are found to be connected with the separation and attachment lines in the skin friction topology. The HVP induces the high local turbulent kinetic energy and Reynolds stress, which are also associated with the streamwise vortices and long streaks with high skin friction magnitudes. In addition, the Falkner-Skan flow over an adiabatic wedge is considered to elucidate the relation between skin friction and surface temperature. From a mathematical standpoint, the derivations in this work are direct applications of the well-established results of differential geometry. Nevertheless, the general forms of these relations particularly including the effects of the surface curvature are new, providing a necessary and rational foundation for further studies of near-wall structures in complex flows.

### ACKNOWLEDGMENTS

This work was supported by the National Natural Science Foundation of China (Grant Nos. 91852205 and 91741101) and by the U.S. National Science Foundation (NSF) under Grant Nos. CNS1513031 and CBET-1706130. T. Liu acknowledges the visiting professorship provided by SUSTech when he did this work during the summer in 2018. Computing resources are provided by the Center for Computational Science and Engineering of Southern University of Science and Technology and by the National Center for Atmospheric Research through Grant Nos. CISEL-P35751014 and CISEL-UDEL0001.

### APPENDIX A: DERIVATION OF EQ. (1)

#### 1. Basic equation

The NS equations for a compressible unsteady viscous flow can be written as<sup>21</sup>

$$\rho \mathbf{a} = -\nabla II - \mu \nabla \times \boldsymbol{\omega}, \quad (\text{A1})$$

where  $\mathbf{a} = D\mathbf{u}/Dt$  is the acceleration,  $\mathbf{u}$  is the fluid velocity,  $\boldsymbol{\omega} = \nabla \times \mathbf{u}$  is the vorticity,  $II = p - \mu\theta$ ,  $p$  is the pressure,  $\rho$  is the density of the fluid,  $\mu_\theta = \zeta + 4\mu/3$  is the longitudinal viscosity,  $\zeta$  is the bulk viscosity,  $\mu$  is the dynamic viscosity, and  $\theta = \nabla \cdot \mathbf{u}$  is the dilation rate. It is assumed that the coefficients  $\zeta$  and  $\mu$  are constants and the body force is zero. The stationary body surface denoted by  $\partial B$  is considered, where the boundary condition is  $[\mathbf{u}]_{\partial B} = 0$ . The subscript  $\partial B$  in the variables and operators denotes those at the surface hereafter. Therefore, on  $\partial B$ , Eq. (A1) is reduced to an on-wall condition

$$[\nabla II]_{\partial B} = -\mu[\nabla \times \boldsymbol{\omega}]_{\partial B}, \quad (\text{A2})$$

where  $[\ ]_{\partial B}$  denotes the quantity on the surface. Taking a dot product of the skin-friction vector  $\boldsymbol{\tau} = \mu \boldsymbol{\omega}_{\partial B} \times \mathbf{n}$  on  $\partial B$  with Eq. (A2) and using Eq. (C1) in which the operator  $\circ$  is taken specifically as the cross product  $\times$ , we have

$$\boldsymbol{\tau} \cdot [\nabla II]_{\partial B} = \mu^2 \mathbf{n} \cdot \left\{ \boldsymbol{\omega}_{\partial B} \times (\nabla_{\partial B} \times \boldsymbol{\omega}_{\partial B}) + \boldsymbol{\omega}_{\partial B} \times \left[ \mathbf{n} \times \frac{\partial \boldsymbol{\omega}}{\partial n} \right]_{\partial B} \right\}. \quad (\text{A3})$$

The right-hand side (RHS) of Eq. (A3) can be further decomposed into more terms to be evaluated next.

In the surface coordinate system, the first term in the RHS of Eq. (A3) is expressed as

$$\boldsymbol{\omega}_{\partial B} \times (\nabla_{\partial B} \times \boldsymbol{\omega}_{\partial B}) = \boldsymbol{\omega}_{\partial B} \times \left( \mathbf{g}^\alpha \times \frac{\partial \boldsymbol{\omega}_{\partial B}}{\partial x^\alpha} \right) = \mathbf{g}^\alpha \frac{\partial \Omega_{\partial B}}{\partial x^\alpha} - \omega_{\partial B}^\alpha \frac{\partial \boldsymbol{\omega}_{\partial B}}{\partial x^\alpha}, \quad (\text{A4})$$

where  $\{\mathbf{g}^\alpha\}$  ( $\alpha = 1, 2$ ) are the local contravariant base vectors of the surface,  $\Omega_{\partial B} = \boldsymbol{\omega}_{\partial B}^2/2 = \boldsymbol{\omega}_{\partial B} \cdot \boldsymbol{\omega}_{\partial B}/2$  is the boundary enstrophy, and  $\omega_{\partial B}^\alpha = \boldsymbol{\omega}_{\partial B} \cdot \mathbf{g}^\alpha$  is the projection of the boundary vorticity in the surface coordinates. Furthermore, the second term in the last equality in Eq. (A4) can be written as

$$\begin{aligned} \omega_{\partial B}^\alpha \frac{\partial \boldsymbol{\omega}_{\partial B}}{\partial x^\alpha} &= \omega_{\partial B}^\alpha \frac{\partial (\omega_{\partial B}^\beta \mathbf{g}_\beta)}{\partial x^\alpha} = \omega_{\partial B}^\alpha \left[ \frac{\partial \omega_{\partial B}^\beta}{\partial x^\alpha} \mathbf{g}_\beta + \omega_{\partial B}^\beta \frac{\partial \mathbf{g}_\beta}{\partial x^\alpha} \right] \\ &= \omega_{\partial B}^\alpha \left[ \frac{\partial \omega_{\partial B}^\beta}{\partial x^\alpha} \mathbf{g}_\beta + \omega_{\partial B}^\beta \Gamma_{\alpha\beta}^\gamma \mathbf{g}_\gamma + \omega_{\partial B}^\beta b_{\alpha\beta} \mathbf{n} \right], \end{aligned} \quad (\text{A5})$$

where  $\Gamma_{\alpha\beta}^\gamma$  is the surface Christoffel symbol and  $b_{\alpha\beta}$  ( $\alpha, \beta = 1, 2$ ) are the coefficients of the surface curvature tensor  $\mathbf{K} = b_{\alpha\beta} \mathbf{g}^\alpha \otimes \mathbf{g}^\beta$ , where  $\otimes$  denotes the tensor product.<sup>44–46</sup> Since  $\mathbf{K}$  is a symmetric tensor, the symmetric relation is  $b_{\alpha\beta} = b_{\beta\alpha} = \mathbf{g}_\alpha \cdot \mathbf{K} \cdot \mathbf{g}_\beta$ , where  $\{\mathbf{g}_\alpha\}$  are the local covariant base vectors. The dual relation is  $\mathbf{g}_\alpha \cdot \mathbf{g}^\beta = \delta_\alpha^\beta$ , where  $\delta_\alpha^\beta$  is the Kronecker delta symbol ( $\delta_\alpha^\beta = 1$  if  $\alpha = \beta$  and  $\delta_\alpha^\beta = 0$   $\alpha \neq \beta$ ). Furthermore, since  $\mathbf{n} \cdot \mathbf{g}_\alpha = 0$  and  $\mathbf{n} \cdot \mathbf{g}^\alpha = 0$  on  $\partial B$ , using Eqs. (A4) and (A5), we have

$$\begin{aligned} \mathbf{n} \cdot [\boldsymbol{\omega}_{\partial B} \times (\nabla_{\partial B} \times \boldsymbol{\omega}_{\partial B})] &= -b_{\alpha\beta} \omega_{\partial B}^\alpha \omega_{\partial B}^\beta = -\boldsymbol{\omega}_{\partial B} \cdot \mathbf{K} \cdot \boldsymbol{\omega}_{\partial B} \\ &= -[\boldsymbol{\omega} \cdot \mathbf{K} \cdot \boldsymbol{\omega}]_{\partial B}. \end{aligned} \quad (\text{A6})$$

The second term on the RHS of Eq. (A3) is

$$\begin{aligned} \boldsymbol{\omega}_{\partial B} \times \left[ \mathbf{n} \times \frac{\partial \boldsymbol{\omega}}{\partial n} \right]_{\partial B} &= \left[ \frac{\partial}{\partial n} \left( \frac{1}{2} \boldsymbol{\omega}^2 \right) \right]_{\partial B} \mathbf{n} - (\boldsymbol{\omega}_{\partial B} \cdot \mathbf{n}) \left[ \frac{\partial \boldsymbol{\omega}}{\partial n} \right]_{\partial B} \\ &= \left[ \frac{\partial \Omega}{\partial n} \right]_{\partial B} \mathbf{n}, \end{aligned} \quad (\text{A7})$$

where the condition  $\boldsymbol{\omega}_{\partial B} \cdot \mathbf{n} = 0$  is applied and  $\Omega = |\boldsymbol{\omega}|^2/2$  denotes the enstrophy. Substitution of Eqs. (A6) and (A7) into Eq. (A3) yields

$$\boldsymbol{\tau} \cdot [\nabla II]_{\partial B} = \mu \left( \mu \left[ \frac{\partial \Omega}{\partial n} \right]_{\partial B} - \boldsymbol{\omega}_{\partial B} \cdot \mathbf{K} \cdot \boldsymbol{\omega}_{\partial B} \right). \quad (\text{A8})$$

Furthermore, by using Eq. (C1), the left-hand side (LHS) of Eq. (A8) is

$$\begin{aligned} \boldsymbol{\tau} \cdot [\nabla II]_{\partial B} &= \mu (\boldsymbol{\omega}_{\partial B} \times \mathbf{n}) \cdot \left( \nabla_{\partial B} p_{\partial B} + \mathbf{n} \left[ \frac{\partial p}{\partial n} \right]_{\partial B} - \mu_\theta \nabla_{\partial B} \theta_{\partial B} \right. \\ &\quad \left. - \mu_\theta \mathbf{n} \left[ \frac{\partial \theta}{\partial n} \right]_{\partial B} \right) \\ &= \boldsymbol{\tau} \cdot \nabla_{\partial B} p_{\partial B} - \mu \mu_\theta (\boldsymbol{\omega}_{\partial B} \times \mathbf{n}) \cdot \nabla_{\partial B} \theta_{\partial B}. \end{aligned} \quad (\text{A9})$$

Therefore, combination of Eqs. (A8) and (A9) yields Eq. (1). When the body force is conservative,  $p$  in Eq. (1) should be replaced by  $p + \varphi$ , where  $\varphi$  is the potential of the body force.

## 2. Oseen flow over a sphere

The steady flow over a sphere at low Reynolds numbers (the Oseen flow) is considered as an example.<sup>22</sup> This problem is considered in the spherical coordinate system  $(r, \theta, \phi)$ , where  $\theta$  and  $\phi$  are the polar and azimuthal angles, respectively, and  $r$  is the radial coordinate. Therefore, the velocity components are the functions of  $r, \theta$ , and  $\phi$ . The axial geometry symmetry gives  $\partial/\partial\phi = 0$  and  $u_\phi = 0$ . For very small Reynolds number ( $Re \ll 1$ ), the asymptotic expansion solution of the NS equations to the order  $O(Re^2)$  is given as

$$\frac{u_r}{u_0} = -\left(1 - \frac{3}{2\tilde{r}} + \frac{1}{2\tilde{r}^3}\right)\cos\theta + ReF_r(\tilde{r}, \theta) + O(Re^2), \quad (A10a)$$

$$\frac{u_\theta}{u_0} = \left(1 - \frac{3}{4\tilde{r}} - \frac{1}{4\tilde{r}^3}\right)\sin\theta + ReF_\theta(\tilde{r}, \theta) + O(Re^2), \quad (A10b)$$

where

$$F_r = -\frac{3}{16}\left(2 - \frac{3}{\tilde{r}} + \frac{1}{\tilde{r}^3}\right)\cos\theta + \frac{3}{32}\left(2 - \frac{3}{\tilde{r}} + \frac{1}{\tilde{r}^2} - \frac{1}{\tilde{r}^3} + \frac{1}{\tilde{r}^4}\right) \times (2 - 3\sin^2\theta), \quad (A11a)$$

$$F_\theta = \left[\frac{3}{32}\left(4 - \frac{3}{\tilde{r}} - \frac{1}{\tilde{r}^3}\right)\sin\theta - \frac{3}{32}\left(4 - \frac{3}{\tilde{r}} + \frac{1}{\tilde{r}^3} - \frac{2}{\tilde{r}^4}\right)\sin\theta\cos\theta\right], \quad (A11b)$$

$\tilde{r} = r/R$ ,  $Re = u_0R/\nu$ ,  $R$  is the radius of the sphere, and  $u_0$  is the freestream velocity along the opposite direction of the  $z$  axis. The vorticity components are  $\omega_r = 0$ ,  $\omega_\theta = 0$ , and

$$\omega_\phi = \frac{u_0}{R}\left[\frac{3\sin\theta}{2\tilde{r}^2} + ReG_\phi(\tilde{r}, \theta)\right] + O(Re^2), \quad (A12)$$

where

$$G_\phi = \frac{9\tilde{r}\sin(2\theta) - 6\sin(2\theta) + 18\tilde{r}^2\sin(\theta) - 27\tilde{r}^2\sin(2\theta) + 12\tilde{r}^3\sin(2\theta)}{32\tilde{r}^4}. \quad (A13)$$

The boundary vorticity is

$$[\omega_\phi]_{\partial B} = \frac{u_0}{R}\left(\frac{3}{2}\sin\theta - Re\left(\frac{3}{8}\sin(2\theta) - \frac{9}{16}\sin\theta\right)\right) + O(Re^2). \quad (A14)$$

The normal derivative of the enstrophy  $\Omega = |\boldsymbol{\omega}|^2/2$  is

$$\frac{\partial\Omega}{\partial n} = \frac{u_0^2}{R^3}\left[-\frac{9\sin^2\theta}{2\tilde{r}^5} + ReH_\Omega(\tilde{r}, \theta) + O(Re^2)\right], \quad (A15)$$

where

$$H_\Omega = -\frac{27\sin^2\theta(4\tilde{r}^3\cos\theta - 12\tilde{r}^2\cos\theta - 4\cos\theta + 5\tilde{r}\cos\theta + 4\tilde{r}^2)}{32\tilde{r}^7}. \quad (A16)$$

From Eq. (A15), we have the BEF

$$\left[\frac{\partial\Omega}{\partial n}\right]_{\partial B} = -\frac{9}{2}\frac{u_0^2}{R^3}\sin^2\theta + Re\frac{u_0^2}{R^3}\frac{27\sin^2\theta(7\cos\theta - 4)}{32} + O(Re^2). \quad (A17)$$

The metric tensor can be expressed as  $\mathbf{I} = g_{ij}\mathbf{g}^i \otimes \mathbf{g}^j = g\langle ij\rangle\mathbf{e}(i) \otimes \mathbf{e}(j)$ , and the coefficients are given by

$$[g_{ij}] = \begin{bmatrix} R^2 & 0 \\ 0 & R^2\sin^2\theta \end{bmatrix}, \text{ and } [g\langle ij\rangle] = \begin{bmatrix} 1 & 0 \\ 0 & 1 \end{bmatrix}, \quad (A18)$$

where  $\{\mathbf{g}^i\}$  ( $i = 1, 2, 3$ ) are the local contravariant base vectors, and  $\{\mathbf{e}(i)\}$  ( $i = 1, 2, 3$ ) are the local unit orthogonal base vectors. Furthermore, we can calculate the curvature tensor  $\mathbf{K} = b_{ij}\mathbf{g}^i \otimes \mathbf{g}^j = b\langle ij\rangle\mathbf{e}(i) \otimes \mathbf{e}(j)$  on the surface of the sphere, where the coefficients are

$$[b_{ij}] = \begin{bmatrix} -R & 0 \\ 0 & -R\sin^2\theta \end{bmatrix}, \text{ and } [b\langle ij\rangle] = \begin{bmatrix} -1/R & 0 \\ 0 & -1/R \end{bmatrix}. \quad (A19)$$

Therefore, the contribution induced by the surface curvature is

$$\begin{aligned} \boldsymbol{\omega}_{\partial B} \cdot \mathbf{K} \cdot \boldsymbol{\omega}_{\partial B} &= -\frac{1}{R}[\omega_\phi]_{\partial B}^2 \\ &= -\frac{9}{4}\frac{u_0^2}{R^3}\sin^2\theta - Re\frac{u_0^2}{R^3}\frac{3\sin(\theta)(9\sin(\theta) - 6\sin(2\theta))}{16} \\ &\quad + O(Re^2). \end{aligned} \quad (A20)$$

Thus, combination of Eqs. (A17) and (A20) yields

$$\mu f_\Omega = \mu^2\frac{u_0^2}{R^3}\left[-\frac{9}{4}\sin^2\theta + Re\frac{9(13\cos\theta - 6)\sin^2\theta}{32}\right] + O(Re^2). \quad (A21)$$

On the other hand, the skin friction vector  $\boldsymbol{\tau} = \mu\boldsymbol{\omega}_{\partial B} \times \mathbf{n}$  is

$$\boldsymbol{\tau} = \mu\frac{u_0}{R}\left[\frac{3}{2}\sin\theta - \left(\frac{3}{8}\sin(2\theta) - \frac{9}{16}\sin\theta\right)Re\right]\mathbf{e}_\theta + O(Re^2), \quad (A22)$$

and the surface pressure gradient  $\nabla_{\partial B}p_{\partial B} = R^{-1}\partial p_{\partial B}/\partial\theta\mathbf{e}_\theta$  is

$$\nabla_{\partial B}p_{\partial B} = \frac{\mu u_0}{R^2}\left[-\frac{3\sin\theta}{2} + \left(\frac{27}{32}\sin(2\theta) - \frac{9}{16}\sin\theta\right)Re\right]\mathbf{e}_\theta + O(Re^2). \quad (A23)$$

From Eqs. (A21)–(A23), it can be confirmed that the relation  $\boldsymbol{\tau} \cdot \nabla_{\partial B}p_{\partial B} = \mu f_\Omega$  holds up to the order of  $O(Re)$ . It is expected that this relation should hold in higher orders.

## 3. Creeping liquid film flow

Another example is a two-dimensional (2D) gravity-driven creeping liquid film flow over a wavy surface. The expansion solution of the Stokes equation using the complex variable was given by Scholle *et al.*,<sup>43</sup> which reveals closed separations (vortices) in a deep wavy wall. We examine whether this 2D solution is consistent with the general theory presented in this paper. For convenience, we adopt the same coordinate system and notations introduced by Scholle *et al.*<sup>43</sup>

In 2D, skin friction can be expressed by the vorticity on a boundary, i.e.,

$$\tilde{\boldsymbol{\tau}}_w = \mu\tilde{\boldsymbol{\omega}}_{\partial B} \times \mathbf{n} = \mu\tilde{\omega}_{y,\partial B}\mathbf{e}_y \times \mathbf{n} = \mu\tilde{\omega}_{y,\partial B}\mathbf{t}, \quad (A24)$$

where  $\mathbf{e}_y$  is the third direction perpendicular to the 2D plane,  $\mathbf{t}$  and  $\mathbf{n}$  are the unit tangent and normal vectors of the boundary curve, respectively, and the overhead “ $\sim$ ” denotes a dimensional quantity. The source term in Eq. (1) is

$$\tilde{f}_\Omega = \mu^2 \left( \left[ \frac{\partial \tilde{\Omega}}{\partial \mathbf{n}} \right]_{\partial B} - \tilde{\omega}_{\partial B} \cdot \mathbf{K} \cdot \tilde{\omega}_{\partial B} \right) = \mu^2 \tilde{\omega}_{y,\partial B} \left[ \frac{\partial \tilde{\omega}_y}{\partial \mathbf{n}} \right]_{\partial B}, \quad (\text{A25})$$

where the quadratic term  $\tilde{\omega}_{\partial B} \cdot \mathbf{K} \cdot \tilde{\omega}_{\partial B}$  vanishes. Therefore, on the boundary curve, Eq. (1) is reduced to

$$\frac{\partial \tilde{p}_{\partial B}}{\partial \tilde{s}} = \mathbf{t} \cdot \tilde{\nabla}_{\partial B} \tilde{p}_{\partial B} = \mu \left[ \frac{\partial \tilde{\omega}_y}{\partial \mathbf{n}} \right]_{\partial B}. \quad (\text{A26})$$

In fact, Eq. (A26) is one of a pair of coupling equations given by Lighthill.<sup>1</sup> The nondimensional coordinates and velocity components are defined as  $(x, z) = (\tilde{x}, \tilde{z})2\pi/\lambda$  and  $(u, w) = (\tilde{u}, \tilde{w})/U$ , respectively, where  $\lambda$  is the wavelength of a wavy surface,  $U = \rho g \lambda^2 \sin \alpha / (8\pi^2 \mu)$  is the characteristic velocity, and  $\alpha$  is the mean inclination angle of the surface. The nondimensional pressure is defined as  $p_{\partial B} = \tilde{p}_{\partial B}(\lambda/2\pi\mu U)$ , where  $2\pi\mu U/\lambda$  is the characteristic pressure. Therefore, the nondimensional form of Eq. (A26) is

$$\frac{\partial p_{\partial B}}{\partial \tilde{s}} = \left[ \frac{\partial \omega_y}{\partial \mathbf{n}} \right]_{\partial B}. \quad (\text{A27})$$

The remaining task is to prove that the solution for the creeping film flow satisfies Eq. (A27).

According to Scholle *et al.*,<sup>43</sup> the stream function is expressed as

$$\psi = h(\xi + \bar{\xi})^2 - \frac{1}{3}(\xi + \bar{\xi})^3 + R(\xi) + (\xi + \bar{\xi})Q(\xi) + \bar{R}(\bar{\xi}) + (\xi + \bar{\xi})\bar{Q}(\bar{\xi}), \quad (\text{A28})$$

where  $\xi = (z + ix)/2$  is a complex variable,  $\bar{\xi} = (z - ix)/2$  is the conjugate variable, and  $R(\xi)$  and  $Q(\xi)$  are complex functions expressed as a Fourier series. The vorticity  $\boldsymbol{\omega} = \nabla \times \mathbf{u}$  is given by

$$\omega_y = \Delta \psi = \frac{\partial^2 \psi}{\partial \xi \partial \bar{\xi}} = 2h - 2(\xi + \bar{\xi}) + \frac{dQ}{d\xi}(\xi) + \frac{d\bar{Q}}{d\bar{\xi}}(\bar{\xi}). \quad (\text{A29})$$

Therefore, the vorticity gradient components are

$$\begin{aligned} \frac{\partial \omega_y}{\partial x} &= \frac{\partial \omega_y}{\partial \xi} \frac{\partial \xi}{\partial x} + \frac{\partial \omega_y}{\partial \bar{\xi}} \frac{\partial \bar{\xi}}{\partial x} = \frac{i}{2} \left( \frac{d^2 Q}{d\xi^2}(\xi) - \frac{d^2 \bar{Q}}{d\bar{\xi}^2}(\bar{\xi}) \right), \\ \frac{\partial \omega_y}{\partial z} &= \frac{\partial \omega_y}{\partial \xi} \frac{\partial \xi}{\partial z} + \frac{\partial \omega_y}{\partial \bar{\xi}} \frac{\partial \bar{\xi}}{\partial z} = -\frac{1}{2} \left( 4 - \frac{d^2 Q}{d\xi^2}(\xi) - \frac{d^2 \bar{Q}}{d\bar{\xi}^2}(\bar{\xi}) \right). \end{aligned} \quad (\text{A30})$$

The hydrodynamic pressure ( $p_h$ ) defined by Scholle *et al.*<sup>43</sup> is

$$p_h = p_s + 2h \cot \alpha - 2z \cot \alpha - i \left[ \frac{dQ}{d\xi}(\xi) - \frac{d\bar{Q}}{d\bar{\xi}}(\bar{\xi}) \right], \quad (\text{A31})$$

where  $p_s$  is the hydrodynamic pressure at the free surface of the liquid film. The gravitational force is  $-\rho \mathbf{g} \cdot \tilde{\mathbf{r}} = -\rho g \tilde{x} \sin \alpha + \rho g \tilde{z} \cos \alpha$ , where  $\tilde{\mathbf{r}} = \tilde{x} \mathbf{e}_x + \tilde{z} \mathbf{e}_z$  is the positional vector. Thus, the nondimensional gravitational force is  $-\rho \mathbf{g} \cdot \mathbf{r} = -2x + 2z \cot \alpha$ . Since the gravitational force can be absorbed into the pressure term, the equivalent nondimensional pressure is written as

$$\begin{aligned} p &= p_h - \rho \mathbf{g} \cdot \mathbf{r} \\ &= p_s + 2h \cot \alpha + i(2\xi - 2\bar{\xi}) - i \left[ \frac{dQ}{d\xi}(\xi) - \frac{d\bar{Q}}{d\bar{\xi}}(\bar{\xi}) \right]. \end{aligned} \quad (\text{A32})$$

Therefore, the pressure gradient components are

$$\begin{aligned} \frac{\partial p}{\partial x} &= \frac{\partial p}{\partial \xi} \frac{\partial \xi}{\partial x} + \frac{\partial p}{\partial \bar{\xi}} \frac{\partial \bar{\xi}}{\partial x} = -\frac{1}{2} \left( 4 - \frac{d^2 Q}{d\xi^2}(\xi) - \frac{d^2 \bar{Q}}{d\bar{\xi}^2}(\bar{\xi}) \right), \\ \frac{\partial p}{\partial z} &= \frac{\partial p}{\partial \xi} \frac{\partial \xi}{\partial z} + \frac{\partial p}{\partial \bar{\xi}} \frac{\partial \bar{\xi}}{\partial z} = \frac{i}{2} \left( \frac{d^2 \bar{Q}}{d\bar{\xi}^2}(\bar{\xi}) - \frac{d^2 Q}{d\xi^2}(\xi) \right). \end{aligned} \quad (\text{A33})$$

For the configuration considered by Scholle *et al.*,<sup>43</sup> the tangent vector and the normal vector of the bottom surface curve  $z = b(x)$  are given as, respectively,

$$\begin{aligned} \mathbf{t} &= [\mathbf{e}_x + b'(x)\mathbf{e}_z] / \sqrt{1 + [b'(x)]^2}, \\ \mathbf{n} &= [-b'(x)\mathbf{e}_x + \mathbf{e}_z] / \sqrt{1 + [b'(x)]^2}, \end{aligned} \quad (\text{A34})$$

where  $b'(x) = db/dx$  is the slope of the bottom surface. Using Eqs. (A30), (A33), and (A34), we have the pressure and vorticity gradients projected on the surface

$$\begin{aligned} \frac{\partial p_{\partial B}}{\partial \tilde{s}} &= \left[ \frac{\partial p}{\partial x} \right]_{\partial B} (\mathbf{t} \cdot \mathbf{e}_x) + \left[ \frac{\partial p}{\partial z} \right]_{\partial B} (\mathbf{t} \cdot \mathbf{e}_z) \\ &= -\frac{1}{2\sqrt{1 + [b'(x)]^2}} \left( 4 - \frac{d^2 Q}{d\xi^2} - \frac{d^2 \bar{Q}}{d\bar{\xi}^2} \right) - \frac{ib'(x)}{2\sqrt{1 + [b'(x)]^2}} \\ &\quad \times \left( \frac{d^2 Q}{d\xi^2} - \frac{d^2 \bar{Q}}{d\bar{\xi}^2} \right) \end{aligned} \quad (\text{A35})$$

and

$$\begin{aligned} \left[ \frac{\partial \omega_y}{\partial \mathbf{n}} \right]_{\partial B} &= \left[ \frac{\partial \omega_y}{\partial x} \right]_{\partial B} (\mathbf{n} \cdot \mathbf{e}_x) + \left[ \frac{\partial \omega_y}{\partial z} \right]_{\partial B} (\mathbf{n} \cdot \mathbf{e}_z) \\ &= \frac{-ib'(x)}{2\sqrt{1 + [b'(x)]^2}} \left( \frac{d^2 Q}{d\xi^2} - \frac{d^2 \bar{Q}}{d\bar{\xi}^2} \right) - \frac{1}{2\sqrt{1 + [b'(x)]^2}} \\ &\quad \times \left( 4 - \frac{d^2 Q}{d\xi^2} - \frac{d^2 \bar{Q}}{d\bar{\xi}^2} \right). \end{aligned} \quad (\text{A36})$$

Since Eq. (A35) equals Eqs. (A36) and (A27) is proven for the gravity-driven creeping liquid flow.

## APPENDIX B: DERIVATION OF EQ. (4)

### 1. Basic equation

The energy equation for a compressible unsteady viscous flow is written as<sup>22</sup>

$$\rho c \left( \frac{\partial T}{\partial t} + \mathbf{u} \cdot \nabla T \right) = -p\theta + \mu \Phi + k \nabla^2 T, \quad (\text{B1})$$

where  $\rho$  is the density of the fluid,  $c$  is the specific heat at constant pressure,  $T$  is the temperature,  $\mathbf{u}$  is the velocity of the fluid,  $p$  is the pressure,  $\theta \equiv \nabla \cdot \mathbf{u}$  is the dilation rate,  $\mu$  is the dynamic viscosity, and  $\Phi$  is the dissipation function. On a stationary surface  $\partial B$ , the no-slip boundary condition  $\mathbf{u}_{\partial B} = 0$  is imposed. The surface temperature  $T_{\partial B} = T_{\partial B}(\mathbf{x}, t)$  is a physical quantity to be determined experimentally or computationally, and it is not given (or imposed) as a Dirichlet boundary condition in this problem. Here, the

incompressible flow with the dilation rate  $\theta = 0$  is considered. Following the conventional notation in differential geometry, we denote  $x^3$  as the normal coordinate from the wall (see Appendix C 2). Differentiating Eq. (B1) with respect to  $x^3$  and using the relation  $\partial \mathbf{u} / \partial x^3 = \mathbf{n} \cdot (\nabla \otimes \mathbf{u})$ , we have the following equation on  $\partial B$ :

$$\begin{aligned} \rho c \left( \frac{\partial}{\partial t} \left[ \frac{\partial T}{\partial x^3} \right]_{\partial B} + [(\mathbf{n} \cdot (\nabla \otimes \mathbf{u})) \cdot (\nabla T)]_{\partial B} \right) \\ = \mu \left[ \frac{\partial \Phi}{\partial x^3} \right]_{\partial B} + k \left[ \frac{\partial}{\partial x^3} \nabla^2 T \right]_{\partial B}. \end{aligned} \quad (\text{B2})$$

For generality, the tensor product notation  $\otimes$  is used in the following derivations in which  $\mathbf{u} \cdot (\nabla \otimes T) \equiv \mathbf{u} \cdot \nabla T$ ,  $\mathbf{u} \cdot (\nabla \otimes \mathbf{u}) \equiv \mathbf{u} \cdot \nabla \mathbf{u}$ , and  $\mathbf{u} \otimes \mathbf{u} \equiv \mathbf{u}\mathbf{u}$  in this case.

The second term on the RHS of Eq. (28) is evaluated. Using the relations

$$\frac{\partial}{\partial x^3} \nabla T = \frac{\partial}{\partial x^3} \left( \mathbf{g}^i \frac{\partial T}{\partial x^i} \right) = \frac{\partial \mathbf{g}^\alpha}{\partial x^3} \frac{\partial T}{\partial x^\alpha} + \nabla \left( \frac{\partial T}{\partial x^3} \right), \quad (\text{B3a})$$

$$\nabla \cdot \left( \frac{\partial}{\partial x^3} \nabla T \right) = \nabla \cdot \left( \frac{\partial \mathbf{g}^\alpha}{\partial x^3} \frac{\partial T}{\partial x^\alpha} \right) + \nabla^2 \left( \frac{\partial T}{\partial x^3} \right), \quad (\text{B3b})$$

we obtain

$$\begin{aligned} \frac{\partial}{\partial x^3} (\nabla^2 T) &= \frac{\partial}{\partial x^3} \left( \mathbf{g}^i \cdot \frac{\partial \nabla T}{\partial x^i} \right) = \frac{\partial \mathbf{g}^\alpha}{\partial x^3} \cdot \frac{\partial \nabla T}{\partial x^\alpha} + \nabla \cdot \left( \frac{\partial \mathbf{g}^\alpha}{\partial x^3} \frac{\partial T}{\partial x^\alpha} \right) \\ &+ \nabla^2 \left( \frac{\partial T}{\partial x^3} \right), \end{aligned} \quad (\text{B4})$$

where  $i = 1, 2, 3$  and  $\alpha = 1, 2$ . Equation (B4) on  $\partial B$  is

$$\begin{aligned} \left[ \frac{\partial}{\partial x^3} (\nabla^2 T) \right]_{\partial B} &= \left[ \frac{\partial \mathbf{g}^\alpha}{\partial x^3} \cdot \frac{\partial \nabla T}{\partial x^\alpha} \right]_{\partial B} + \left[ \nabla \cdot \left( \frac{\partial \mathbf{g}^\alpha}{\partial x^3} \frac{\partial T}{\partial x^\alpha} \right) \right]_{\partial B} \\ &+ \left[ \nabla^2 \left( \frac{\partial T}{\partial x^3} \right) \right]_{\partial B}. \end{aligned} \quad (\text{B5})$$

Furthermore, we calculate the three terms of the RHS of Eq. (B5). The first term is

$$\begin{aligned} \left[ \frac{\partial \mathbf{g}^\alpha}{\partial x^3} \cdot \frac{\partial \nabla T}{\partial x^\alpha} \right]_{\partial B} &= b_{\beta}^{\alpha} \mathbf{g}^{\beta} \cdot \frac{\partial [\nabla T]_{\partial B}}{\partial x^\alpha} \\ &= b_{\beta}^{\alpha} \mathbf{g}^{\beta} \cdot \frac{\partial}{\partial x^\alpha} \left( \nabla_{\partial B} T_{\partial B} + \mathbf{n} \left[ \frac{\partial T}{\partial x^3} \right]_{\partial B} \right) \\ &= b_{\beta}^{\alpha} \mathbf{g}^{\beta} \cdot \frac{\partial \nabla_{\partial B} T_{\partial B}}{\partial x^\alpha} - \mathbf{K} : \mathbf{K} \left[ \frac{\partial T}{\partial x^3} \right]_{\partial B} \\ &= \text{Tr}(\nabla_{\partial B} \nabla_{\partial B} T_{\partial B} \cdot \mathbf{K}) - \mathbf{K} : \mathbf{K} \left[ \frac{\partial T}{\partial x^3} \right]_{\partial B}, \end{aligned} \quad (\text{B6})$$

where  $\text{Tr}(\mathbf{S}) = \mathbf{g}_\alpha \cdot \mathbf{S} \cdot \mathbf{g}^\alpha$ ,  $\mathbf{K} : \mathbf{K} = b_{\alpha\beta} b^{\alpha\beta}$ , and  $b_{\beta}^{\alpha} = g^{\alpha\gamma} b_{\gamma\beta}$ . To evaluate the second term of the RHS of Eq. (B5), using the relations

$$\left[ \frac{\partial \mathbf{g}^\alpha}{\partial x^3} \frac{\partial T}{\partial x^\alpha} \right]_{\partial B} = b_{\beta}^{\alpha} \mathbf{g}^{\beta} \frac{\partial T_{\partial B}}{\partial x^\alpha} = \mathbf{K} \cdot \nabla_{\partial B} T_{\partial B}, \quad (\text{B7a})$$

$$\nabla_{\partial B} \cdot \left[ \frac{\partial \mathbf{g}^\alpha}{\partial x^3} \frac{\partial T}{\partial x^\alpha} \right]_{\partial B} = (\nabla_{\partial B} \cdot \mathbf{K}) \cdot (\nabla_{\partial B} T_{\partial B}) + \text{Tr}(\nabla_{\partial B} \nabla_{\partial B} T_{\partial B} \cdot \mathbf{K}), \quad (\text{B7b})$$

$$\begin{aligned} \mathbf{n} \cdot \left[ \frac{\partial}{\partial x^3} \left( \frac{\partial \mathbf{g}^\alpha}{\partial x^3} \frac{\partial T}{\partial x^\alpha} \right) \right]_{\partial B} &= \mathbf{n} \cdot \left[ \frac{\partial^2 \mathbf{g}^\alpha}{\partial (x^3)^2} \right]_{\partial B} \frac{\partial T_{\partial B}}{\partial x^\alpha} \\ &+ \mathbf{n} \cdot b_{\beta}^{\alpha} \mathbf{g}^{\beta} \frac{\partial}{\partial x^\alpha} \left[ \frac{\partial T}{\partial x^3} \right]_{\partial B} = 0, \end{aligned} \quad (\text{B7c})$$

we obtain

$$\begin{aligned} \left[ \nabla \cdot \left( \frac{\partial \mathbf{g}^\alpha}{\partial x^3} \frac{\partial T}{\partial x^\alpha} \right) \right]_{\partial B} &= \nabla_{\partial B} \cdot \left[ \frac{\partial \mathbf{g}^\alpha}{\partial x^3} \frac{\partial T}{\partial x^\alpha} \right]_{\partial B} + \mathbf{n} \cdot \left[ \frac{\partial}{\partial x^3} \left( \frac{\partial \mathbf{g}^\alpha}{\partial x^3} \frac{\partial T}{\partial x^\alpha} \right) \right]_{\partial B} \\ &= (\nabla_{\partial B} \cdot \mathbf{K}) \cdot (\nabla_{\partial B} T_{\partial B}) + \text{Tr}(\nabla_{\partial B} \nabla_{\partial B} T_{\partial B} \cdot \mathbf{K}). \end{aligned} \quad (\text{B8})$$

The third term of the RHS of Eq. (B5) is evaluated below. Applying Eq. (C1), we have

$$\left[ \nabla^2 \frac{\partial T}{\partial x^3} \right]_{\partial B} = \nabla_{\partial B} \cdot \left[ \nabla \frac{\partial T}{\partial x^3} \right]_{\partial B} + \mathbf{n} \cdot \left[ \frac{\partial}{\partial x^3} \left( \nabla \frac{\partial T}{\partial x^3} \right) \right]_{\partial B}. \quad (\text{B9})$$

By applying Eq. (C1) again, the first term in the RHS of Eq. (B9) becomes

$$\begin{aligned} \nabla_{\partial B} \cdot \left[ \nabla \frac{\partial T}{\partial x^3} \right]_{\partial B} &= \nabla_{\partial B}^2 \left[ \frac{\partial T}{\partial x^3} \right]_{\partial B} + (\nabla_{\partial B} \cdot \mathbf{n}) \left[ \frac{\partial^2 T}{\partial (x^3)^2} \right]_{\partial B} \\ &+ \mathbf{n} \cdot \nabla_{\partial B} \left[ \frac{\partial^2 T}{\partial (x^3)^2} \right]_{\partial B} \\ &= \nabla_{\partial B}^2 \left[ \frac{\partial T}{\partial x^3} \right]_{\partial B} - 2H_{\text{mean}} \left[ \frac{\partial^2 T}{\partial (x^3)^2} \right]_{\partial B}, \end{aligned} \quad (\text{B10})$$

where  $H_{\text{mean}} = (\kappa_1 + \kappa_2)/2 = -\nabla_{\partial B} \cdot \mathbf{n}/2 = \text{tr}(\mathbf{K})/2$  is the mean curvature with the principal curvatures  $\kappa_1$  and  $\kappa_2$  and  $\mathbf{K} = b_{\alpha\beta} \mathbf{g}^\alpha \otimes \mathbf{g}^\beta$  is the curvature tensor. Similarly, the second term on the RHS of Eq. (B9) is

$$\begin{aligned} \mathbf{n} \cdot \left[ \frac{\partial}{\partial x^3} \left( \nabla \frac{\partial T}{\partial x^3} \right) \right]_{\partial B} &= \mathbf{n} \cdot \left[ \mathbf{K} \cdot \nabla_{\partial B} \left[ \frac{\partial T}{\partial x^3} \right]_{\partial B} + \nabla_{\partial B} \left[ \frac{\partial^2 T}{\partial (x^3)^2} \right]_{\partial B} \right. \\ &\left. + \mathbf{n} \left[ \frac{\partial^3 T}{\partial (x^3)^3} \right]_{\partial B} \right] = \left[ \frac{\partial^3 T}{\partial (x^3)^3} \right]_{\partial B}. \end{aligned} \quad (\text{B11})$$

Substitution of Eqs. (B10) and (B11) into Eq. (B9) yields

$$\left[ \nabla^2 \frac{\partial T}{\partial x^3} \right]_{\partial B} = \nabla_{\partial B}^2 \left[ \frac{\partial T}{\partial x^3} \right]_{\partial B} - 2H_{\text{mean}} \left[ \frac{\partial^2 T}{\partial (x^3)^2} \right]_{\partial B} + \left[ \frac{\partial^3 T}{\partial (x^3)^3} \right]_{\partial B}. \quad (\text{B12})$$

The use of Eqs. (B6), (B8), and (B12) yields

$$\begin{aligned} \left[ \frac{\partial}{\partial x^3} (\nabla^2 T) \right]_{\partial B} &= -\mathbf{K} : \mathbf{K} \left[ \frac{\partial T}{\partial x^3} \right]_{\partial B} + 2 \text{Tr}(\nabla_{\partial B} \nabla_{\partial B} T_{\partial B} \cdot \mathbf{K}) \\ &+ (\nabla_{\partial B} \cdot \mathbf{K}) \cdot (\nabla_{\partial B} T_{\partial B}) + \nabla_{\partial B}^2 \left[ \frac{\partial T}{\partial x^3} \right]_{\partial B} \\ &- 2H_{\text{mean}} \left[ \frac{\partial^2 T}{\partial (x^3)^2} \right]_{\partial B} + \left[ \frac{\partial^3 T}{\partial (x^3)^3} \right]_{\partial B}. \end{aligned} \quad (\text{B13})$$

Equation (B13) indicates that the normal derivative of the 3D diffusion term on  $\partial B$  is decomposed into the quasi-2D diffusion on  $\partial B$ , the curvature terms of the thermal diffusion, and the higher-order term.

The second term of the LHS of Eq. (B2) is evaluated next. We notice the relation

$$\begin{aligned} \left[ \frac{\partial \mathbf{u}}{\partial x^3} \right]_{\partial B} &= \mathbf{n} \cdot [\nabla \otimes \mathbf{u}]_{\partial B} = [\mathbf{u} \otimes \nabla]_{\partial B} \cdot \mathbf{n} \\ &= [\mathbf{u} \otimes \nabla - \nabla \otimes \mathbf{u}]_{\partial B} \cdot \mathbf{n} + [\nabla \otimes \mathbf{u}]_{\partial B} \cdot \mathbf{n} \\ &= \omega_{\partial B} \times \mathbf{n} + [\nabla \otimes \mathbf{u}]_{\partial B} \cdot \mathbf{n}. \end{aligned} \quad (B14)$$

The final equality of Eq. (B14) has the two terms. The first term is evaluated based on the property of the rotation tensor. By using Eq. (C1), the second term is

$$\begin{aligned} (\nabla \otimes \mathbf{u})_{\partial B} \cdot \mathbf{n} &= \left( \nabla_{\partial B} \otimes \mathbf{u}_{\partial B} + \mathbf{n} \otimes \left[ \frac{\partial \mathbf{u}}{\partial x^3} \right]_{\partial B} \right) \cdot \mathbf{n} \\ &= \left( \mathbf{n} \otimes \left[ \frac{\partial (u^\alpha \bar{\mathbf{g}}_\alpha + u^3 \mathbf{n})}{\partial x^3} \right]_{\partial B} \right) \cdot \mathbf{n} = \left[ \frac{\partial u^3}{\partial x^3} \right]_{\partial B} \mathbf{n}. \end{aligned} \quad (B15)$$

For an incompressible flow with  $\theta = 0$ , we observe

$$\begin{aligned} \theta_{\partial B} &= [\nabla \cdot \mathbf{u}]_{\partial B} = \nabla_{\partial B} \cdot \mathbf{u}_{\partial B} + \mathbf{n} \cdot \left[ \frac{\partial \mathbf{u}}{\partial x^3} \right]_{\partial B} \\ &= \mathbf{n} \cdot \left( \omega_{\partial B} \times \mathbf{n} + \left[ \frac{\partial u^3}{\partial x^3} \right]_{\partial B} \mathbf{n} \right) = \left[ \frac{\partial u^3}{\partial x^3} \right]_{\partial B} = 0. \end{aligned} \quad (B16)$$

The use of Eqs. (B14)–(B16) yields

$$\begin{aligned} (\mathbf{n} \cdot (\nabla \otimes \mathbf{u})_{\partial B}) \cdot (\nabla T)_{\partial B} &= (\omega_{\partial B} \times \mathbf{n}) \cdot \left( \nabla_{\partial B} T_{\partial B} + \mathbf{n} \left[ \frac{\partial T}{\partial x^3} \right]_{\partial B} \right) \\ &= \frac{\boldsymbol{\tau}}{\mu} \cdot \nabla_{\partial B} T_{\partial B}. \end{aligned} \quad (B17)$$

Re-arrangement of Eq. (B2) by using Eqs. (B13) and (B17) leads to Eq. (4).

It is noted that the term  $\nabla_{\partial B} \nabla_{\partial B} T_{\partial B}$  in Eq. (B13) is expressed as

$$\begin{aligned} \nabla_{\partial B} \nabla_{\partial B} T_{\partial B} &= \mathbf{g}^\beta \frac{\partial}{\partial x^\beta} \left( \mathbf{g}^\alpha \frac{\partial T_{\partial B}}{\partial x^\alpha} \right) = \mathbf{g}^\beta \left( \frac{\partial \mathbf{g}^\alpha}{\partial x^\beta} \frac{\partial T_{\partial B}}{\partial x^\alpha} + \mathbf{g}^\alpha \frac{\partial^2 T_{\partial B}}{\partial x^\alpha \partial x^\beta} \right) \\ &= \frac{\partial^2 T_{\partial B}}{\partial x^\alpha \partial x^\beta} \mathbf{g}^\alpha \otimes \mathbf{g}^\beta - \Gamma_{\beta\gamma}^\alpha \frac{\partial T_{\partial B}}{\partial x^\alpha} \mathbf{g}^\beta \otimes \mathbf{g}^\gamma + \frac{\partial T_{\partial B}}{\partial x^\alpha} b_{\beta\alpha}^\alpha \mathbf{g}^\beta \otimes \mathbf{n}. \end{aligned} \quad (B18)$$

For a flat surface where  $\mathbf{g}^\alpha = \mathbf{e}(\alpha)$  and  $\mathbf{g}^\beta = \mathbf{e}(\beta)$  in the Cartesian coordinate system, both the Christoffel symbols  $\Gamma_{\beta\gamma}^\alpha$  and the curvature tensor  $b_{\beta\alpha}^\alpha$  are zero. In this case, it is reduced to the Hessian matrix, i.e.,

$$\nabla_{\partial B} \nabla_{\partial B} T_{\partial B} = \frac{\partial^2 T_{\partial B}}{\partial x^\alpha \partial x^\beta} \mathbf{g}^\alpha \otimes \mathbf{g}^\beta = \frac{\partial^2 T_{\partial B}}{\partial x^\alpha \partial x^\beta} \mathbf{e}(\alpha) \otimes \mathbf{e}(\beta). \quad (B19)$$

For a curved surface, the curvature effect and the derivative of the temperature along the coordinate curve are coupled in the two additional terms.

## 2. Falkner-Skan flow over an adiabatic wedge

The Falkner-Skan flow is considered as an example of heat transfer. A wedge with an adiabatic wall is placed in a 2D uniform steady-state incompressible flow with a constant temperature at large Reynolds numbers. The external velocity over the wedge is  $U(x) = a_0 x^m$ ,  $x$  is the coordinate on the wedge surface from the wedge leading edge,  $m$  is a power-law component, and  $a_0$  is a positive constant.<sup>22</sup> The half angle is given by  $\pi\beta/2$ , where  $\beta = 2m/(m+1)$ . The velocity can be represented as

$$u = U(x)f'(\eta) = a_0 x^m f'(\eta), \quad (B20a)$$

$$v = -\sqrt{\frac{m+1}{2}} \nu a_0 x^{m-1} \left( f + \frac{m-1}{m+1} \eta f' \right), \quad (B20b)$$

where the similarity variable  $\eta = y\sqrt{(m+1)a_0 x^{m-1}/2\nu}$ ,  $y$  is the wall-normal coordinate,  $f$  is a function of  $\eta$ , and  $\nu$  is the kinematic viscosity. The similarity equation and boundary conditions for  $f$  are

$$f''' + ff'' + \beta(1-f'^2) = 0, \quad (B21a)$$

$$f(0) = 0, f'(0) = 0, f'(\infty) = 1. \quad (B21b)$$

Then, the skin friction vector can be evaluated as

$$\boldsymbol{\tau} = \mu \boldsymbol{\omega} \times \mathbf{n} = \mu \left( \sqrt{\frac{m+1}{2}} \frac{a_0}{\nu} a_0 x^{\frac{3m-1}{2}} f''(0) \right) \mathbf{e}_x. \quad (B22)$$

The temperature can be written as  $T = T_\infty + U(x)^2 \Theta/2c$ , where  $\Theta$  satisfies the following similarity equation with the boundary conditions on the adiabatic surface and infinity

$$Pr^{-1} \Theta'' + f \Theta' - 2\beta f' \Theta = -2f''^2, \quad (B23a)$$

$$\Theta'(0) = 0, \Theta(\infty) = 0, \quad (B23b)$$

where  $Pr = \nu/a$  is the Prandtl number and  $a = k/\rho c$  is the thermal diffusivity. Using Eqs. (B21)–(B23), we have

$$\left[ \frac{\partial^3 T}{\partial y^3} \right]_{y=0} = \frac{a_0^2 x^{2m}}{2c} Pr(\Theta(0) + 2) 2\beta f''(0) \left( \frac{m+1}{2} \frac{a_0}{\nu} x^{m-1} \right)^{3/2}, \quad (B24a)$$

$$\left[ \frac{\partial \Phi}{\partial y} \right]_{y=0} = -2\beta U^2 f''(0) \left( \frac{m+1}{2} \frac{a_0}{\nu} x^{m-1} \right)^{3/2}, \quad (B24b)$$

$$\boldsymbol{\tau} \cdot \nabla_{\partial B} T_{\partial B} = \frac{\mu}{c} \Theta(0) f''(0) m a_0^3 \sqrt{\frac{m+1}{2}} \frac{a_0}{\nu} x^{\frac{7m-3}{2}}. \quad (B24c)$$

Therefore, combining Eqs. (B24a)–(B24b), we validate Eq. (4) that has the following special form:

$$\boldsymbol{\tau} \cdot \nabla_{\partial B} T_{\partial B} = \mu \frac{k}{\rho c} \left( \frac{\partial^3 T}{\partial y^3} \right)_{y=0} + \frac{\mu^2}{\rho c} \left( \frac{\partial \Phi}{\partial x^3} \right)_{y=0}, \quad (B25)$$

where the surface curvature terms vanish in the Falkner-Skan flow. The corresponding mass-transfer problem in the Falkner-Skan flow is considered. In a 2D uniform steady-state incompressible

flow, the binary mass diffusion equation (6) without a source term has the same form as the energy equation (B1), when temperature  $T$  and the thermal diffusivity  $a = k/\rho c$  are replaced by the relative concentration  $\phi = \rho_1/\rho$  and the diffusivity of a binary system  $D_{12}$ , respectively. The distribution of the relative concentration of the species 1 can be written as  $\phi = \phi_\infty + U(x)^2 \Theta_m / 2U_{ref}^2$ , where  $U_{ref}$  is a reference velocity. The similarity equation for  $\Theta_m$  are the same as Eq. (B23a) when the Prandtl number  $Pr = \nu/a$  is replaced by the Schmidt number  $Sc = \nu/D_{12}$ . The boundary conditions at the surface and infinity remain the same, i.e.,  $\Theta_m'(0) = 0$ ,  $\Theta_m(\infty) = 0$ . Since the solution structure is the same for the mass-transfer and heat-transfer problems, Eq. (7) can be validated in the Falkner-Skan flow.

## APPENDIX C: USEFUL RESULTS IN DIFFERENTIAL GEOMETRY

### 1. Decomposition of gradient operator on a surface

We introduce a useful lemma stated as follows. For a tensor field  $\Psi$  that is defined in a neighborhood of the surface  $\partial B$ , the following relation holds, i.e.,

$$[\nabla \circ \Psi]_{\partial B} = \nabla_{\partial B} \circ \Psi_{\partial B} + \left[ \mathbf{n} \circ \frac{\partial \Psi}{\partial n} \right]_{\partial B}, \quad (C1)$$

where  $\mathbf{n}$  is the normal unit vector of the surface,  $\partial \Psi / \partial n$  is the normal derivative of  $\Psi$  on the surface, and the notation  $\circ$  represents any reasonable product operator such as the dot product  $\cdot$ , the cross product  $\times$ , and the tensor product  $\otimes$ . In particular, if  $\Psi$  is a scalar field,  $\nabla \Psi$  means the gradient of the scalar field in a three-dimensional (3D) Euclidean space and  $\nabla_{\partial B} \Psi_{\partial B}$  means the gradient of the scalar field tangent to the surface. This lemma is proved below.

For any surface coordinate system, a point on the surface is represented by  $\mathbf{x} = (x^1, x^2)$ . We can construct a 3D spatial curvilinear coordinate system  $(\mathbf{x}, x^3) = (x^1, x^2, x^3)$  based on the surface coordinate system. According to the mathematical properties of the coordinate system described in Appendix A 2, the gradient operator  $\nabla$  in the coordinate system is expressed as

$$\nabla = \bar{\mathbf{g}}^i(\mathbf{x}, x^3) \frac{\partial}{\partial x^i} = \bar{\mathbf{g}}^1(\mathbf{x}, x^3) \frac{\partial}{\partial x^1} + \bar{\mathbf{g}}^2(\mathbf{x}, x^3) \frac{\partial}{\partial x^2} + \mathbf{n}(\mathbf{x}) \frac{\partial}{\partial x^3}, \quad (C2)$$

where  $\{\bar{\mathbf{g}}^i\}$  ( $i = 1, 2, 3$ ) are the local contravariant base vectors under the 3D spatial curvilinear coordinate system  $(\mathbf{x}, x^3)$ . Also, the surface gradient operator  $\nabla_{\partial B}$  in the surface coordinate system  $\mathbf{x} = (x^1, x^2)$  can be expressed as  $\nabla_{\partial B} = \mathbf{g}^\alpha(\mathbf{x}) \partial / \partial x^\alpha$  ( $\alpha = 1, 2$ ). Using Eq. (C2), when the operators  $\circ$  and  $\partial / \partial x^i$  are exchangeable, we have

$$\begin{aligned} [\nabla \circ \Psi]_{\partial B} &= \left[ \left( \bar{\mathbf{g}}^i(\mathbf{x}, x^3) \frac{\partial}{\partial x^i} \right) \circ \Psi \right]_{\partial B} \\ &= \left[ \bar{\mathbf{g}}^\alpha(\mathbf{x}, x^3) \circ \frac{\partial \Psi}{\partial x^\alpha} + \mathbf{n}(\mathbf{x}) \circ \frac{\partial \Psi}{\partial x^3} \right]_{\partial B} \\ &= \nabla_{\partial B} \circ \Psi_{\partial B} + \left[ \mathbf{n} \circ \frac{\partial \Psi}{\partial n} \right]_{\partial B}. \end{aligned} \quad (C3)$$

### 2. Geometric properties of a surface

As illustrated in Fig. 8(a), the positional vector of a point on the surface is given by  $\mathbf{r}_s = \mathbf{r}_s(\mathbf{x}) = \mathbf{r}_s(x^1, x^2)$ , where  $\mathbf{x} \in D_s \subset \mathbb{R}^2$

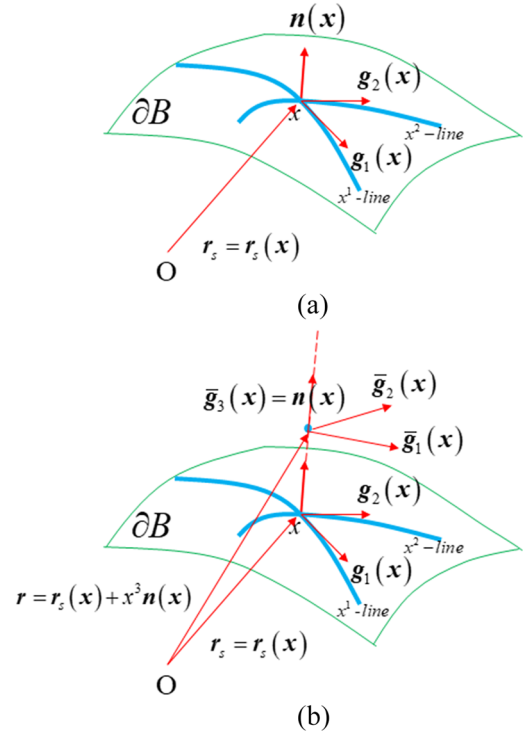


FIG. 8. The surface coordinate system: (a) the positional vector of a point on the surface and (b) any point in the neighborhood of the surface.

are the curvilinear coordinates of the surface. For any fixed point on the surface, there exist two parameterized curves called the  $x^1$ -curve and  $x^2$ -curve passing through it, respectively. Along the  $x^1$ -curve, the coordinate  $x^2$  is fixed, while the coordinate  $x^1$  varies. Similarly, the coordinate  $x^1$  is fixed, while the coordinate  $x^2$  varies along the  $x^2$ -curve. The local covariant base vectors are defined as  $\mathbf{g}_\alpha(\mathbf{x}) = \partial \mathbf{r}_s(\mathbf{x}) / \partial x^\alpha$  ( $\alpha = 1, 2$ ), where  $\mathbf{g}_1$  and  $\mathbf{g}_2$  are tangent to the  $x^1$  curve and  $x^2$ -curve, respectively. Then, the normal unit vector of the surface at the point  $\mathbf{x}$  can be defined as  $\mathbf{n} = \mathbf{g}_1 \times \mathbf{g}_2 / \|\mathbf{g}_1 \times \mathbf{g}_2\|$ . Also, the local contravariant base vectors  $\{\mathbf{g}^\alpha\}$  are defined, which satisfy the condition  $\mathbf{g}^\alpha \cdot \mathbf{g}_\beta = \delta_\alpha^\beta$  ( $\alpha, \beta = 1, 2$ ), where  $\delta_\alpha^\beta$  is the Kronecker delta symbol ( $\delta_\alpha^\beta = 1$  if  $\alpha = \beta$  and  $\delta_\alpha^\beta = 0$   $\alpha \neq \beta$ ). Then, the metric tensor can be defined as  $\mathbf{I} = g_{\alpha\beta} \mathbf{g}^\alpha \otimes \mathbf{g}^\beta$ , where  $g_{\alpha\beta} = \mathbf{g}_\alpha \cdot \mathbf{g}_\beta$  and  $g^{\alpha\beta} = \mathbf{g}^\alpha \cdot \mathbf{g}^\beta$ . It can be proved that  $\mathbf{I}$  is symmetric, i.e.,  $g_{\alpha\beta} = g_{\beta\alpha}$ .

In order to measure the curvature of the surface, the curvature tensor  $\mathbf{K} = b_{\alpha\beta} \mathbf{g}^\alpha \otimes \mathbf{g}^\beta$ , where  $b_{\alpha\beta} = \mathbf{n} \cdot \partial \mathbf{g}_\beta / \partial x^\alpha$  ( $\alpha, \beta = 1, 2$ ).  $\mathbf{K}$  is also a symmetric tensor with  $b_{\beta\alpha} = b_{\alpha\beta}$ . The equations of motion of the base vectors in differential geometry are

$$\begin{aligned} \frac{\partial \mathbf{g}_\alpha}{\partial x^\beta} &= \Gamma_{\alpha\beta}^\gamma \mathbf{g}_\gamma + b_{\alpha\beta} \mathbf{n}, \\ \frac{\partial \mathbf{n}}{\partial x^\alpha} &= -b_{\alpha\gamma} \mathbf{g}^\gamma, \\ \frac{\partial \mathbf{g}^\alpha}{\partial x^\beta} &= -\Gamma_{\beta\gamma}^\alpha \mathbf{g}^\gamma + b_{\beta\alpha}^\alpha \mathbf{n}, \end{aligned} \quad (C4)$$

where  $b_{\beta}^{\alpha} = g^{\alpha\gamma} b_{\gamma\beta}$  and  $\Gamma_{\alpha\beta}^{\gamma} = \partial g_{\alpha}^{\gamma} / \partial x^{\beta} \cdot \mathbf{g}^{\gamma}$  ( $\alpha, \beta, \gamma = 1, 2$ ) is called the Christoffel symbol.

In differential geometry, a 3D curvilinear coordinate system can be reconstructed based on the surface coordinate system. As shown in Fig. 8(b), any point in the neighborhood of the surface can be described as  $\mathbf{r} = \mathbf{r}_s(\mathbf{x}) + x^3 \mathbf{n}(\mathbf{x})$ ,<sup>45</sup> where  $(\mathbf{x}, x^3) \in D_s \times (-\delta, \delta) \subset \mathbb{R}^3$ , and  $\delta$  is a positive constant number. This 3D coordinate system also has its own local covariant base vectors and local contravariant base vectors, which are defined as  $\bar{\mathbf{g}}_i(\mathbf{x}) = \partial \mathbf{r}(\mathbf{x}) / \partial x^i$  and  $\bar{\mathbf{g}}^i \cdot \bar{\mathbf{g}}_j = \delta_j^i$  ( $i, j = 1, 2, 3$ ). Then, we have the following expression:

$$\begin{cases} \bar{\mathbf{g}}_i(\mathbf{x}, x^3) = (\delta_i^j - x^3 b_i^j) \mathbf{g}_j(\mathbf{x}) \\ \bar{\mathbf{g}}_3(\mathbf{x}, x^3) = \mathbf{n}(\mathbf{x}) \end{cases} \quad (i, j = 1, 2), \quad (C5)$$

$$\begin{cases} \bar{\mathbf{g}}^i(\mathbf{x}, x^3) = \frac{(1 - 2x^3 H_{mean}) \delta_i^k + x^3 b_i^k}{1 - 2x^3 H_{mean} + (x^3)^2 K_{Gauss}} \mathbf{g}^k(\mathbf{x}) \\ \bar{\mathbf{g}}^3(\mathbf{x}, x^3) = \mathbf{n} \end{cases} \quad (i, k = 1, 2), \quad (C6)$$

where  $H_{mean} = (\kappa_1 + \kappa_2)/2$  is the mean curvature and  $K_{Gauss} = \kappa_1 \kappa_2$  is the Gaussian curvature. When these base vectors are restricted on the surface, they are the same as local surface base vectors, i.e.,

$$\begin{cases} \bar{\mathbf{g}}_{\alpha}(\mathbf{x}, x^3 = 0) = \mathbf{g}_{\alpha}(\mathbf{x}) \\ \bar{\mathbf{g}}_3(\mathbf{x}, x^3 = 0) = \mathbf{n}(\mathbf{x}) \end{cases} \quad (\alpha = 1, 2), \quad (C7)$$

$$\begin{cases} \bar{\mathbf{g}}^{\alpha}(\mathbf{x}, x^3 = 0) = \mathbf{g}^{\alpha}(\mathbf{x}) \\ \bar{\mathbf{g}}^3(\mathbf{x}, x^3 = 0) = \mathbf{n}(\mathbf{x}) \end{cases} \quad (\alpha = 1, 2). \quad (C8)$$

Therefore, we have

$$\nabla = \bar{\mathbf{g}}^i(\mathbf{x}, x^3) \frac{\partial}{\partial x^i} = \bar{\mathbf{g}}^{\alpha}(\mathbf{x}, x^3) \frac{\partial}{\partial x^{\alpha}} + \mathbf{n}(\mathbf{x}) \frac{\partial}{\partial x^3} \quad (\alpha = 1, 2), \quad (C9)$$

$$\nabla_{\partial B} = \mathbf{g}^{\alpha}(\mathbf{x}) \frac{\partial}{\partial x^{\alpha}} = \mathbf{g}^1(\mathbf{x}) \frac{\partial}{\partial x^1} + \mathbf{g}^2(\mathbf{x}) \frac{\partial}{\partial x^2} \quad (\alpha = 1, 2). \quad (C10)$$

REFERENCES

<sup>1</sup>M. J. Lighthill, in *Introduction of Boundary Layer Theory in Laminar Boundary Layers*, edited by L. Rosenhead (Oxford University Press, Oxford, UK, 1963), pp. 46–113.  
<sup>2</sup>J. C. R. Hunt, C. J. Abell, J. A. Peterka, and H. Woo, “Kinematical studies of the flows around free or surface-mounted obstacles; applying topology to flow visualization,” *J. Fluid Mech.* **86**, 179–200 (1978).  
<sup>3</sup>M. Tobak and D. J. Peake, “Topology of three-dimensional separation flows,” *Annu. Rev. Fluid Mech.* **14**, 61–85 (1982).  
<sup>4</sup>A. E. Perry and M. S. Chong, “A series-expansion study of the Navier-Stokes equations with applications to three-dimensional separation patterns,” *J. Fluid Mech.* **173**(11), 207–223 (1986).  
<sup>5</sup>J. Z. Wu, R. W. Tramel, F. L. Zhu, and X. Y. Yin, “A vorticity dynamics theory of three-dimensional flow separation,” *Phys. Fluids* **12**, 1932–1954 (2000).  
<sup>6</sup>J. M. Deléry, “Robert Legendre and Henri Werle: Toward the elucidation of three-dimensional separation,” *Annu. Rev. Fluid Mech.* **33**, 129–154 (2001).  
<sup>7</sup>J. F. Foss, “Surface selections and topological constraint evaluations for flow field analyses,” *Exp. Fluids* **37**, 883–897 (2004).  
<sup>8</sup>E. H. Hirschel, J. Cousteix, and W. Kordulla, in *Three-Dimensional Attached Viscous Flows* (Springer, Berlin, 2014), Chap. 7.

<sup>9</sup>U. Dallmann, “Topological structures of three-dimensional flow separation,” DFVLR Report No. IB 221-82 A 07, Göttingen, Germany, 1983.  
<sup>10</sup>A. E. Perry and M. S. Chong, “A description of eddying motions and flow patterns using critical-point concepts,” *Annu. Rev. Fluid Mech.* **19**, 125–155 (1987).  
<sup>11</sup>T. Bewley and B. Protas, “Skin friction and pressure: The “footprints” of turbulence,” *Physica D* **196**(1-2), 28–44 (2004).  
<sup>12</sup>A. Surana, O. Grunberg, and G. Haller, “Exact theory of three-dimensional flow separation. Part 1. Steady separation,” *J. Fluid Mech.* **564**, 57–103 (2006).  
<sup>13</sup>T. Liu, T. Misaka, K. Asai, S. Obayashi, and J. Z. Wu, “Feasibility of skin-friction diagnostics based on surface pressure gradient field,” *Meas. Sci. Technol.* **27**, 125304 (2016).  
<sup>14</sup>T. Liu, S. Wang, and G. He, “Explicit role of viscosity in generating lift,” *AIAA J.* **55**(11), 3990–3994 (2017).  
<sup>15</sup>T. Liu, “Skin-friction and surface-pressure structures in near-wall flows,” *AIAA J.* **56**(10), 3887–3896 (2018).  
<sup>16</sup>T. Liu and S. Woodiga, “Feasibility of global skin friction diagnostics using temperature sensitive paint,” *Meas. Sci. Technol.* **22**, 115402 (2011).  
<sup>17</sup>M. Miozzi, A. Capone, F. Di Felice, C. Klein, and T. Liu, “Global and local skin friction diagnostics from TSP surface patterns on an underwater cylinder in cross flow,” *Phys. Fluids* **28**, 124101 (2016).  
<sup>18</sup>T. Liu, S. Woodiga, J. Gregory, and J. Sullivan, “Global skin friction diagnostics based on surface mass-transfer visualizations,” *AIAA J.* **52**, 2369–2383 (2014).  
<sup>19</sup>T. Liu, M. H. Makhmalbaf, R. S. V. Ramasamy, S. Kode, and P. Merati, “Skin friction fields and surface dye patterns on delta wings in water flows,” *J. Fluids Eng.* **137**, 071202-1–071202-14 (2015).  
<sup>20</sup>W. H. Chen, *Differential Geometry* (Peking University Press, Beijing, 2006).  
<sup>21</sup>J. Z. Wu, H. Y. Ma, and M. D. Zhou, *Vorticity and Vortex Dynamics* (Springer, Berlin, 2006).  
<sup>22</sup>H. Schlichting and K. Gersten, *Boundary-Layer Theory*, 9th ed. (Springer, Berlin, 2017).  
<sup>23</sup>L. C. Burmeister, in *Convective Heat Transfer*, 2nd ed. (Wiley, New York, 1993), Chap. 2.  
<sup>24</sup>B. K. Horn and B. G. Schunck, “Determining optical flow,” *Artif. Intell.* **17**(1-3), 185–204 (1981).  
<sup>25</sup>T. Liu and L. Shen, “Fluid flow and optical flow,” *J. Fluid Mech.* **614**, 253–291 (2008).  
<sup>26</sup>G. Aubert and P. Kornprobst, “A mathematical study of the relaxed optical flow problem in the space  $BV(\Omega)$ ,” *SIAM J. Math. Anal.* **30**, 1282–1308 (1999).  
<sup>27</sup>G. Aubert, R. Deriche, and P. Kornprobst, “Computing optical flow via variational techniques,” *SIAM J. Appl. Math.* **60**, 156–182 (1999).  
<sup>28</sup>B. Wang, Z. Cai, L. Shen, and T. Liu, “An analysis of physics-based optical flow method,” *J. Comput. Appl. Math.* **276**, 62–80 (2015).  
<sup>29</sup>A. N. Tikhonov and V. Y. Arsenin, in *Solutions of Ill-Posed Problems* (Wiley, New York, 1977), Chap. II.  
<sup>30</sup>C. W. Groetsch, in *Inverse Problems in the Mathematical Sciences* (Vieweg Braunschweig, 1993), Chap. 5.  
<sup>31</sup>S. J. Kline, W. C. Reynolds, F. A. Schraub, and P. W. Runstadler, “The structure of turbulent boundary layers,” *J. Fluid Mech.* **30**, 741–773 (1967).  
<sup>32</sup>M. R. Head and P. Bandyopadhyay, “New aspects of turbulent boundary-layer structure,” *J. Fluid Mech.* **107**, 297–338 (1981).  
<sup>33</sup>S. K. Robinson, “Coherent motions in the turbulent boundary layer,” *Annu. Rev. Fluid Mech.* **23**, 601–639 (1991).  
<sup>34</sup>J. Jiménez, “Coherent structures in wall-bounded turbulence,” *J. Fluid Mech.* **842**, P1–P100 (2018).  
<sup>35</sup>R. J. Adrian, C. D. Meinhardt, and C. D. Tomkins, “Vortex organization in the outer region of the turbulent boundary layer,” *J. Fluid Mech.* **422**, 1–54 (2000).  
<sup>36</sup>K. T. Christensen and R. J. Adrian, “Statistical evidence of hairpin vortex packets in wall turbulence,” *J. Fluid Mech.* **431**, 433–443 (2001).  
<sup>37</sup>P. Moin and J. Kim, “The structure of the vorticity field in turbulent channel flow. Part 1. Analysis of instantaneous fields and statistical correlations,” *J. Fluid Mech.* **155**, 441–464 (1985).

- <sup>38</sup>J. Zhou, R. J. Adrian, S. Balachandar, and T. M. Kendall, "Mechanisms for generating coherent packets of hairpins in channel flow," *J. Fluid Mech.* **387**, 353–396 (1999).
- <sup>39</sup>X. Wu and P. Moin, "Direct numerical simulation of turbulence in a nominally zero-pressure-gradient flat-plate boundary layer," *J. Fluid Mech.* **630**, 5–41 (2009).
- <sup>40</sup>G. Eitel-Amor, R. Örlü, P. Schlatter, and O. Flores, "Hairpin vortices in turbulent boundary layers," *Phys. Fluids* **27**, 025108 (2015).
- <sup>41</sup>C. Peng, "Study of turbulence modulation by finite size solid particles with the lattice Boltzmann method," Ph.D. thesis, University of Delaware, Delaware, 2018.
- <sup>42</sup>L.-P. Wang, G. Peng, Z. L. Guo, and Z. S. Yu, "Flow modulation by finite-size neutrally buoyant particles in a turbulent channel flow," *ASME J. Fluids Eng.* **138**, 041306 (2016).
- <sup>43</sup>M. Scholle, A. Wierschem, and N. Aksel, "Creeping films with vortices over strongly undulated bottoms," *Acta Mech.* **168**(3), 167–193 (2004).
- <sup>44</sup>S. S. Chern, W. H. Chen, and K. S. Lam, *Lectures on Differential Geometry* (World Scientific Pub Co, Inc., Singapore, 1999).
- <sup>45</sup>K. Z. Huang, *Tensor Analysis* (Tsinghua University Press, Beijing, 2003).
- <sup>46</sup>X. L. Xie, *Modern Tensor Analysis with Applications in Continuum Mechanics* (Fudan University Press, Shanghai, 2014).